BONE TISSUE GENERATION ON BIODEGRADABLE POLYMERIC SCAFFOLD

A THESIS SUBMITTED TO
THE GRADUATE SCHOOL OF NATURAL AND APPLIED SCIENCES
OF
THE MIDDLE EAST TECHNICAL UNIVERSITY

BY

GAMZE TORUN KÖSE

IN PARTIAL FULFILLMENT OF THE REQUIREMENTS FOR THE DEGREE OF
DOCTOR OF PHILOSOPHY
IN
THE DEPARTMENT OF BIOTECHNOLOGY

JANUARY 2002

Approval of the Graduate School of Natural and Applied Sciences

Prof. Dr. Tayfur ÖZTÜRK
Director

I certify that this thesis satisfies all the requirements as a thesis for the degree of Doctor of Philosophy.

Prof. Dr. Ayhan Sıtkı DEMİR
Head of Department

This is to certify that we have read this thesis and that in our opinion it is fully adequate, in scope and quality, as a thesis for the degree of Doctor of Philosophy in Biotechnology.

Prof. Dr. Feza KORKUSUZ
Co-Supervisor

Prof. Dr. Vasıf HASIRCI
Supervisor

Examining Committee Members

Prof. Dr. Hüseyin Avni ÖKTEM

Prof. Dr. Mesude İŞCAN

Assoc. Prof. Dr. Aykut ÖZKUL

Asst. Prof. Dr. Ayşegül ÇETIN

Prof. Dr. Vasıf HASIRCI

ABSTRACT

BONE TISSUE GENERATION ON BIODEGRADABLE POLYMERIC SCAFFOLDS

Torun Köse, Gamze

Ph.D., Department of Biotechnology

Supervisor: Prof. Dr. Vasıf Hasırcı

Co-Supervisor: Prof. Dr. Feza Korkusuz

January 2002, 144 pages

In the present study, tissue engineered bone was produced on calcium phosphate loaded collagen and PHBV8 matrices. Osteoblasts isolated from rat bone marrow were characterized by light microscopy, alkaline phosphatase (ALP) activity, osteocalcin determination assay, and Western blots for integrin. Population doubling time of the cells was found as 50 ± 2 h at 37 °C in a CO_2 incubator. PHBV8 foams

were treated with rf-oxygen plasma to modify their surface chemistry and hydrophilicity to increase the reattachment of osteoblasts. Optimum power and duration was found to be 100 W 10 min. Another carrier material, lyophilized collagen foam, was loaded with calcium phosphate to mimic the composition of the bone to provide a better environment for cell proliferation and also to prevent rapid resorption of the foam. The presence of calcium phosphate and the molar ratio of calcium over phosphorus (2.26) in the collagen matrix was determined by SEM-EDS. The surface characteristics, average pore size and distribution in PHBV8 and collagen matrices were studied by SEM and Scion Image Analysis Program. Void volume and density of the foams were also found to be related to foam preparation conditions. Stability of PHBV foams in aqueous media was studied. The weight and density were unchanged for a period of 120 days but then a significant decrease was observed for the rest of the study.

In order to determine the cell density of the films and the foams, MTS assay was carried out. Osteoblast growth inside the matrices was also determined by ALP and osteocalcin assays, Western blot for integrin, along with histological examinations, SEM and confocal microscopy. After 29 days of incubation, growth of osteoblasts on matrices and initiation of mineralization were observed. Large size sucrose (300-500 μm) loaded PHBV8 (6 %, w/w) foams treated with 100 W 10 min rf-plasma were found to be the most suitable matrices for osteoblast growth.

Keywords: Bone tissue engineering, biomaterials, biodegradability, PHBV8 collagen

ÖZ

BİYOBOZUNUR POLİMERİK MATRİKSLER ÜZERİNDE KEMİK DOKUSU OLUŞUMU

Torun Köse, Gamze

Doktora, Biyoteknoloji Bölümü

Tez Yöneticisi: Prof. Dr. Vasıf Hasırcı

Ortak Tez Yöneticisi: Prof. Dr. Feza Korkusuz

Ocak 2002, 144 pages

Bu çalışmada, kalsiyum fosfat yüklü kollajen ve poli(hidroksibütirat-ko-hidroksivalerat) (PHBV8) matrikslerinde doku mühendisliği yöntemleri kullanarak kemik dokusu üretilmiştir. Sıçan kemik iliğinden izole edilen osteoblastlar ışık mikroskobu, alkalen fosfataz (ALP) aktivitesi, osteokalsin tayin deneyi ve integrin için uygulanan Western blot ile karakterize edilmiştir. Hücre

sayılarının 37 °C de CO_2 inkübatöründe ikiye katlanma süresi 50 ± 2 saat olarak bulunmuştur. PHBV8 süngerlerinin hidrofilisite ve yüzey kimyasal özelliklerini değiştirmek ve osteoblastların tutunma düzeyini artırmak için de rf-oksijen plazması uygulanmıştır. Optimum güç ve zaman 100 W 10 dk olarak bulunmuştur. Başka bir taşıyıcı malzeme, lyofilize kollajen, kemik kimyasal yapısını taklit edebilmek ve bu yolla daha iyi hücre artışı sağlayabilmek ve ayrıca matriks malzemesinin hızlı resorpsiyonunu önleyebilmek için kalsiyum fosfat yüklenmiştir. Kalsiyum fosfatın varlığı ve kalsiyumun fosfora molar oranı (2.26) SEM-EDS ile saptanmıştır. PHBV8 ve kollajen matrikslerinin yüzey özellikleri, ortalama gözenek boyutları ve dağılımları, SEM ve SCION görüntü analizi programı ile incelenmiştir. Hazırlama koşullarına bağlı olarak matrikslerdeki boşlukların hacmi ve yoğunlukları da bulunmuştur. PHBVnin sıvı ortamdaki kararlılığı da incelenmiştir. 120 gün boyunca ağırlık ve yoğunluk değişmemiş ancak çalışmanın geri kalan kısmında oldukça belirgin bir düşme gözlenmiştir.

Film ve matrikslerdeki hücre yoğunluğunun belirlenmesi için MTS testi kullanılmıştır. Matrikslerin içindeki osteoblast gelişimi ALP, osteokalsin testi, integrin için uygulanan Western blot, histolojik deneyler, SEM ve konfokal mikroskop ile belirlenmiştir. 29 gün inkübasyondan sonra matrikslerde osteoblastların büyüdüğü ve mineralizasyonun başladığı görülmüştür. Büyük boyutlu sükroz (300-500 μm) ile yüklü, 100 W 10 dakika rf-plazmayla etkileştirilmiş PHBV8'in (6%, w/w) osteoblast büyümesi için en uygun matriks olduğu görülmüştür.

Anahtar Kelimeler: Kemik doku mühendisliği, biyomateryaller, biyobozunurluk, PHBV8, kollajen

Dedicated to my daughter, Melike

ACKNOWLEDGEMENT

I would like to express my deepest gratitude to Prof. Dr. Vasıf HASIRCI and Prof. Dr. Feza KORKUSUZ for their valuable guidance, encouragements and patience throughout this study.

I am especially indepted to Assoc. Prof. Dr. Aykut ÖZKUL for his valuable and continued support during my studies.

I am grateful to Prof. Dr. Gabriel LOPEZ-BERESTEIN for providing me a wonderful opportunity to master tissue culture techniques during my stay in Houston, Texas, USA.

I am grateful to Suzan BER and Halime KENAR for their kind contribution to the experimental part of work.

I would like to thank Prof. Dr. Nesrin HASIRCI for rf-oxygen plasma modification of the matrices, Asst. Prof. Dr. Petek KORKUSUZ for histological evaluations, Assoc. Prof. Dr. Serhat AKIN for his guidance in surface analysis, Assoc. Prof. Dr. Metin ALABAY for the sterilization of matrix materials, Assoc. Prof. Dr. Nuhan PURALİ for confocal microscopy studies and Dr. Nusret TAHERİ for osteocalcin determination experiment.

I would like to thank Graduate School of Natural and Applied Sciences for the support they provided (Project Number: AFP-2000-07-02-00-07.).

I would like to thank all my friends, Dr. Fatma KÖK, Dr. Türker BARAN, Dr. Dilek ŞENDİL, Dr. Ayşen TEZCANER, Süleyman COŞKUN, Sibel ÇINAR, Özlem ÇİRLİ, Deniz YÜCEL, Gözde YÜCEL, and our technician Zeynel AKIN for their support in this research.

I am also deeply grateful to my mother Sevim TORUN and sister Pınar TORUN for their understanding and continued support during my study. Without their support, this work would never have been completed.

Finally, I would like to express my appreciation to my husband Murat KÖSE for his deep love and continued support.

GAMZE TORUN KÖSE

TABLE OF CONTENTS

LIST OF TABLES

Tables

LIST OF FIGURES

Figures

LIST OF ABBREVIATIONS

Ab :	Antibody
ACP :	Acid phosphatase
ALP :	Alkaline phosphatase
BSA :	Bovine serum albumin
BMP :	Bone morphogenic protein
DBM :	Demineralized bone matrix
DMEM :	Dulbecco's Minimal Eagle medium
ECM :	Extracellular matrix
FCS :	Fetal calf serum
FGF :	Fibroblast growth factor
HA :	Hydroxyapatite
IGF :	Insulin-like growth factor
kGy :	Kilo Gray
MTS :	3-(4,5-dimethylthiazol-2-yl)-5-(3carboxymethoxyphenyl)-2-(4-sulfophenyl)-2H- tetrazolium, (Owen's reagent)
OP :	Oxygen plasma treatment
PBS :	Phosphate buffer saline
PDGF :	Platelet derived growth factor

PEG :	Polyethylene glycol
PGA :	Poly(glycolic acid)
PHA :	Poly(hydroxyalkanoate)
PHB :	Poly(hydroxybutyrate)
PHBV :	Poly(3-hydroxybutyrate-co-3-hydroxyvalerate)
PHBV8 :	Poly(3-hydroxybutyrate-co-3-hydroxyvalerate) containing 8% by mole of hydoxyvalerate
PLLA :	Poly(L-lactic acid)
PLGA :	Poly(lactic-co-glycolic acid)
PMS :	Phenazine methosulfate
PPF :	Poly(propylene fumarate)
PS :	Polystyrene
rf :	Radiofrequency
RT :	Room temperature
SDS :	Sodium dodecyl sulfate
SEM :	Scanning electron microscope
SEM-EDS :	Scanning electron microscope coupled with energy dispersive spectroscopy
TCP :	Tricalcium phosphate
TCPs :	Tissue culture grade polystyrene
TGF-β :	Transforming growth factor- beta
Trypsin-EDTA :	Trypsin-ethylenediamine tetraacetic acid

CHAPTER 1

INTRODUCTION

1.1. Tissue Engineering

Tissue engineering is the concept that the repair and regeneration of biological tissues can be guided through application and control of cells, materials, and chemoactive proteins (Figure 1.1). It began with the use of active biomaterials; materials designed to interact with the body to encourage tissue repair. It is still an emerging technology (Vacanti et al., 1995) and encompasses the interrelated fields such as chemical engineering, material science and cell biology. The approach is to harvest a relatively small piece of tissue, remove the cells and increase the cell population, seed the cells on a carrier material and generate a substantial amount of tissue by reimplanting the cell-polymer composite. This form of therapy differs from standard therapies in that the engineered tissue becomes integrated within the patient, affording a potentially permanent and specific cure of the disease state. Tissue engineering requires the reformation of an extracellular matrix. The main components of the extracellular matrix are collagen and proteoglycan. In contrast to

proteoglycans, which can be thought as the ground substance, collagens primarily provide stress resistance to tissues.

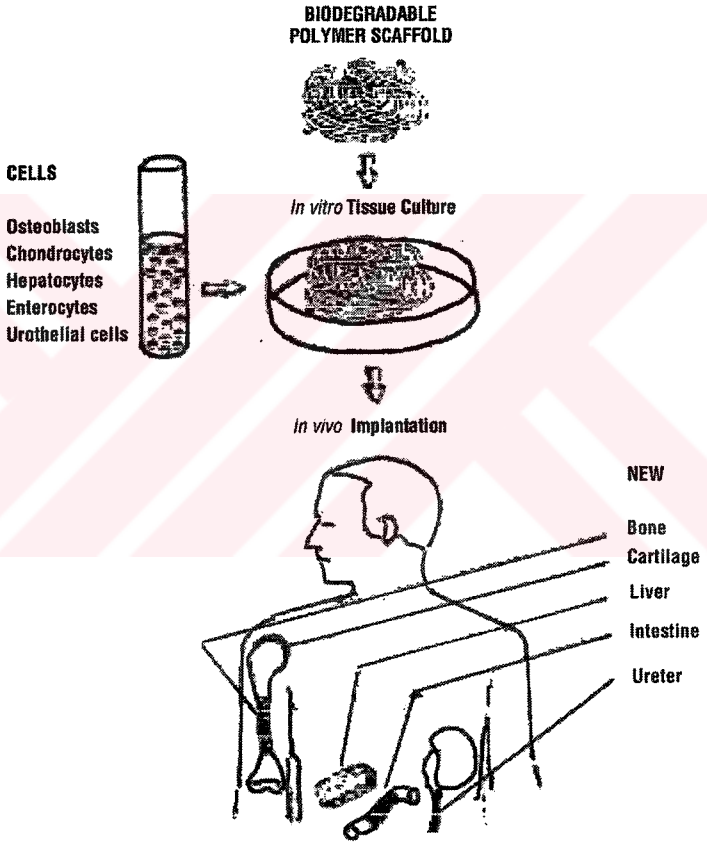

Figure 1.1. A scheme of production of tissue engineered organs. One of the major approaches in tisssue engineering, three-dimensional, highly porous scaffolds composed of synthetic polymers serve as cell transplant devices (from Langer, 1997).

Current tissue engineering approaches commonly use cell attachment scaffolds that are complex composites of naturally occurring extracellular matrix (ECM) molecules (e.g. collagens, glycosaminoglycan), or decellularized biological matrices produced by means of enzymatic or detergent treatments (Bader et al., 1998) which would closely mimic the native cellular environment or synthetic biomaterials (polyurethanes, α-hydroxyacids, ceramics, etc). The control of material properties (e.g. strength, degradation profile, porosity, surface properties and microstructure), ease and reproducibility of fabrication make them good candidates for tissue engineered constructs (Vacanti and Langer, 1999).

1.2. Importance of Carrier Materials in Tissue Engineering

It has been known for a long time that cells differ in their ability to grow and differentiate depending on both the chemistry and mechanics of their ECM substratum. *In vitro*, epithelial cells commonly express more differentiated functions when grown on immobilized ECM molecules (e.g. collagen, fibronectin, and laminin) compared to tissue culture plastic alone. These cells function even better when maintained on specialized artificial basement membrane substrata such as Matrigel® (a complex of different basement membrane molecules that commonly support cell differentiation) (Ingber et al., 1993).

Unfortunately, these artificial ECMs have limitations from an engineering standpoint. They exhibit a limited range of structural and chemical properties and can not be easily chemically modified. Also their large-scale

fabrication can be limited by batch to batch variability caused by the purification step of ECM preparation. The alternative approach for cell transplantation is to develop a completely synthetic attachment foundation that can support a high degree of cell function and yet be highly biocompatible. To accomplish this objective, recent advances in ECM biology must be merged with new developments in bioengineering and polymer chemistry (Ingber, 1993).

In order to select appropriate biomaterials for tissue engineering, it is necessary to understand their influence on cell viability, growth and function. Matrices should be biocompatible (non-carcinogenic, non-toxic, non-allergic, hemocompatible), inert (low or negligible toxicity of degradation products in terms of both and systemic response), reproducibly produced in large quantities, economically feasible and able to maintain its properties in the biological medium. They also should have a sound engineering design and the desired physical and mechanical properties that adequately address short-term function and do not interfere with long-term function.

These matrix materials guide cell organization and growth allowing diffusion of nutrients to the transplanted cells (Pollok and Vacanti, 1996). They also allow vascularization. Vascularization could be a natural host response to the implant or could be artificially induced by sustained release of angiogenic factors from the scaffold. After varying times in culture, they are implanted. Vascular ingrowth, remodeling and regeneration occur *in vivo*, forming a new tissue composed of donor and recipient element. Structural tissues such as skin, bone and cartilage are the most easily produced organs by tissue engineering methods due to their relative simplicity.

1.3. Bone Tissue Engineering

Bone tissue engineering is designed to mimic natural process of bone repair. Bone repair is an attractive and natural target for tissue engineering. Tissue engineering of bone requires three important elements. These are cellular components, extracellular matrices and scaffolds, and growth and differentiation factors. Cells can be obtained from an exogenous source or they can be recruited from the local environment. Scaffold matrix must provide a substrate for cellular attachment, proliferation and differentiation. Growth and differentiation factors must guide the appropriate development of the cellular components.

1.3.1. Bone

Bone is a complex, highly organized, living organ undergoing continuous remodeling throughout life. It contains a large amount of organic material (40%) (Freed and Vunjak-Novakovic 1998). 90-96% of this organic material is collagen, predominantly type 1 along with small amounts of types V and XII, and the rest (4-10%) is bone specific proteoglycans and non-collagenous proteins such as osteocalcin, osteonectin, bone sialoprotein, and bone phosphoproteins. Most of the inorganic matrix or mineral phase of the bone is the crystal of an apatite of calcium and phosphate. This gives bone stiffness and strength. Within this crystal structure other mineral ions such as citrate, carbonate, fluoride and hydroxyl ions also exist. Bone plays a very important role as a primary reservoir of calcium in the body and

exchanges this mineral readily with the extracellular fluid environment (Seal et al. 2001). Also, the hematopoietic marrow, which supplies nutrient-carrying red blood cells and infection-fighting white blood cells, is located in the trabecular bone. Another function of bone is its mechanical role in supporting the tissues and in providing sites for attachment for the muscles that affect body movement and locomotion.

Bones can be classified according to their shape in three groups: short, flat and long bones (Yaszemski et al. 1996a). Short bones such as tarsals, carpals, and vertebral bodies, have thin cortices and are trapezoidal, cuboidal, or irregular in shape. Flat bones have one dimension. While the larger flat bones form the cranial vault, the wing of the ileum, and the scapula, the smaller ones form the lamina of a vertebra. Long bones or tubular bones such as femur, tibia, humerus, metacarpals, metatarsals, and phalanges are usually made of spongy and compact bone. The spongy bone consists of three-dimensional branching of trabeculae interdispersed by bone marrow. The spongy bone changes gradually into compact bone toward the middle of the bone. Cortical (compact) and cancellous (trabecular) bones are the two important bone tissues having the same matrix composition and structure. Cortical bone has a greater density or less porosity than the cancellous bone. Cortical bone forms approximately 80% of the mature skeleton and surrounds the marrow and the cancellous bone plates (Figure 1.2). In long bones, cortical bones form the diaphysis (Buckwalter et al., 1995). The metaphyses contain most of the cancellous bone. The cortical bone decreases in thickness from the mid-part of the diaphysis to the metaphysis where the cancellous bones are arranged to support the subchondral bone. In long bones, cortical bone provides the maximum resistance to torsion and

bending. However, cancellous bone allows great deformation under the same load. Cortical bone also protects the articular cartilage and subchondrial bone from damage by absorbing the impact loads applied across synovial joints. Cancellous bone has approximately twenty times more surface area per unit of volume than does cortical bone and has a higher rate of metabolic activity and remodeling. It can respond more rapidly to changes in mechanical loads than does cortical bone (Figure 1.3). The external and internal surface of the bone is called periosteum and endosteum, respectively, and both have osteogenic properties. Periosteum is primarily affected from the diseases, deformities, injuries of the skeleton, and most orthopedic treatments. It contributes an important part of the blood supply to the bone. Periostal cells can resorb and form bone in response to local or systemic stimuli. During bone growth, they secrete the organic matrix that enlarges the diameter of the bone.

Some tendons and ligaments are inserted primarily into the outer layer of the periosteum. Bone marrow is found in the internal part of the bone and serves as a source of bone cells. The blood vessels in the marrow form a critical part of the circulatory system in bone. Bone cells originate from a mesenchymal stem-cell line (e.g. undifferentiated cells (preosteoblasts), osteoblasts, bone lining cells (osteocytes) and a hematopoietic stem-cell line (e.g. marrow monocytes, preosteoclasts, and osteoclasts).

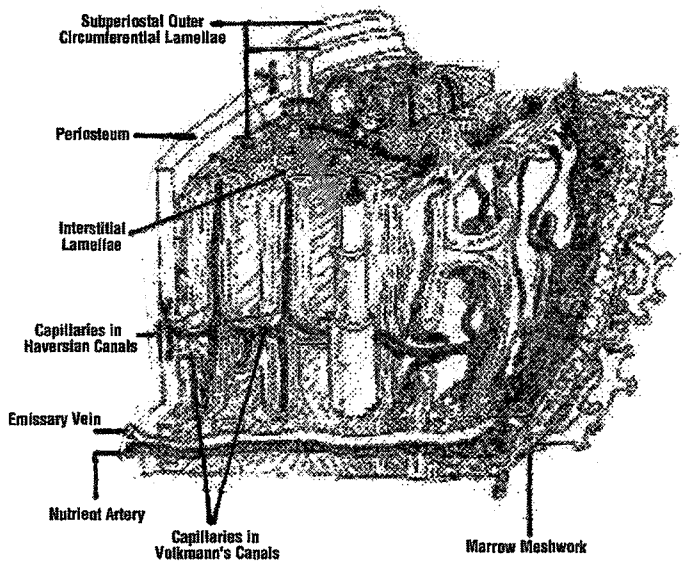

Figure 1.2. The structure of cortical bone (Seal, 2001).

Osteoblasts are differentiated cells, usually derived from osteoprogenitor cells. They are mobile, change shape and size with different rates of matrix production. They appear with the vascular tissue. The main function of the osteoblasts is the synthesis and secretion of the organic matrix of bone. They also control electrolyte fluxes between the extracellular fluid and the osseous fluid and may influence the mineralization of bone matrix through the synthesis of organic matrix components of bone and the production of matrix vesicles. Moreover, some systemic hormones such as parathyroid hormone and local cytokines may stimulate osteoblasts to release mediators that activate osteoclasts (Buckwalter et al. 1995).

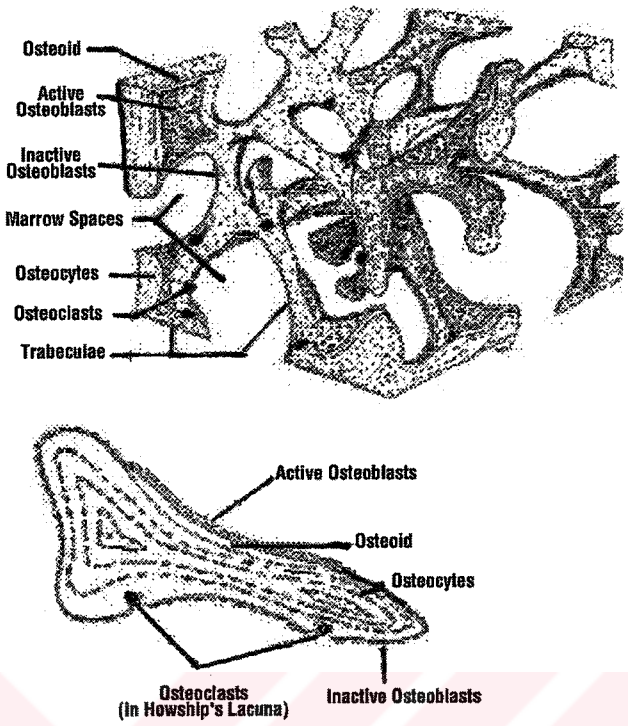

Figure 1.3. a) The structure of trabecular or cancellous bone, b) A more detailed drawing of trabecula (Seal, 2001).

Bone-lining cells lie against the bone matrix and when exposed to parathyroid hormone, they contract and secrete enzymes that remove the thin layer of osteoid. This event permits osteoclasts to attach and resorb the surface of bone. Osteocytes are the most abundantly found bone cells in the mature human skeleton. They surround themselves with an organic matrix and cover the matrix together with the periostal and endosteal cells. Osteoclasts have a very efficient method for destroying bone matrix. They are rarely found in normal bone. Osteoclast precursor cells are found in the marrow or the circulating blood. Stem cells are activated by

specific hormones and growth factors to become osteoclast precursors. When osteoclasts are active, they require great amount of energy to resorb bone.

Bone resorption and bone formation are the two main events of remodeling process, with two well-differentiated cell types, osteoclasts, osteoblasts and their precursors (Figure 1.4). The first step is activation that involves resting osteoblasts or lining cells as well as osteoclast precursors. In the resorption phase, the osteoclasts remove bone to produce Howship's lacunae in trabecular bone or Haversian canals in cortical bone. After osteoclastic resorption is complete, mononuclear cells are seen in the reversal phase and may form the cement line. Thereafter, osteoblast precursors migrate to the bone surface and lay down new matrix in the formation phase.

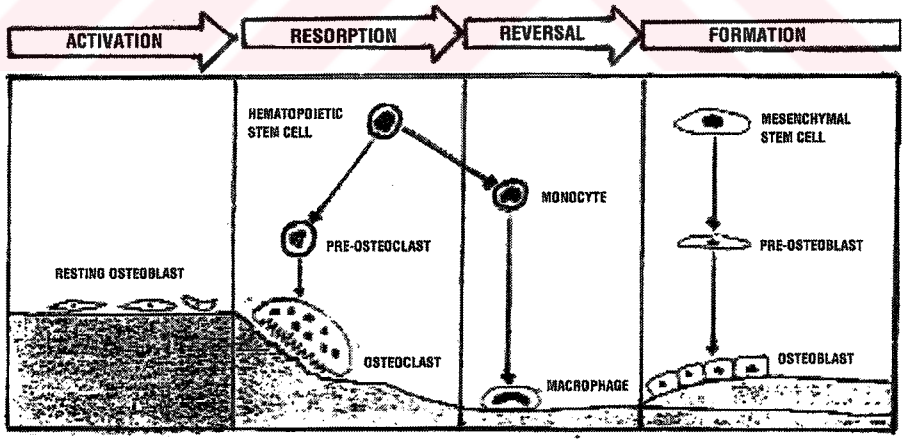

Figure 1.4. The bone remodelling cycle (Raisz, 1988).

Bone cell function is regulated at both the systemic and the local level. Factors that control local formation and resorption of bone such as cytokines, prostaglandins, and mechanical loading have the potential for the treatment of acute fractures, delayed unions, non-unions, and skeletal deformity as well as to enhance the stabilization of joint implants in the skeleton (Raisz 1988).

1.3.2. Matrix Materials Used in Bone Tissue Engineering

Organ or tissue failure or loss is an expensive problem in health care. When the mechanical function of bone is lost by injury, infection, disease or inadequate fracture management, it can only be regained by restoring skeletal continuity at the location of interest. In these situations, the patient suffers from the loss of mechanical support of the body's tissues and loss of muscle attachment sites. Such skeletal defects, therefore, require therapeutic intervention to restore the bone to its proper form. Currently, major approaches to tissue or organ loss are surgical reconstruction, transplantation and artificial prosthesis. Although these therapies have saved and improved countless lives, they remain imperfect solutions. Surgical reconstruction and artificial prosthesis can result in infection, chronic irritation, lack of mechanisms of biological repair and long term problems like development of malignant tumor or calcification of graft. Transplantation is currently limited by increasing donor shortages. Also immunosuppression is required with its serious side effects. Existing autogenous graft materials may play an important role in healing nonunion defects. However, they generally have poor morphologies and interconnectivities that are dissimilar to cancellous bone. They have also limited

resource that leads to donor site morbidity. This may impair their population with cells and vascularization. Allograft bone can also be a successful procedure. Allograft bone has a porous structure and contains some growth factors such as insulin like growth factor, transforming growth factor-β, platelet-derived growth factor, fibroblast growth factor, and BMPs embedded in the bone matrix. These growth factors make allograft bone potentially osteoinductive (Fleming et al., 2000). Allograft bone is fully resorbable, biocompatible and does not have reactive degradation by-products. However its high cost, risk of bacterial or viral infection, and donor-to-donor variation in quality are the major disadvantages of allograft bone.

Various synthetic alternatives such as metals, ceramics and polymers have been tried for many years. However, they have had limited success due to lack of living cells and slow vascularization (Pollok and Vacanti, 1996).

Bone tissue engineering can be addressed to solve the problems such as high cost, risk of bacterial or viral infection, donor shortage, donor-to-donor variation in quality and slow vascularization, etc. For loss of bone or its function, ready-made pliable tissue constructs are very promising. For a successful application of such tissues, the development of biomaterials with suitable mechanical characteristics and degradation behaviour is very important. To minimize a loss of cells, it might be of advantage to preform the biomaterial matrix to a needed shape.

Osteoconductive matrices are fashioned from biodegradable materials of natural origin like collagen, gelatin, hyaluronic acid etc., biodegradable polymers like poly(3-hdroxybutyric acid-co-3-hydroxyvaleric acid) (PHBV), or most commonly from synthetic polymers such as polylactic acid (PLA), polyglycolic acid (PGA), poly(lactic-co-glycolic acid) (PLGA), etc. The matrices used as scaffolds

should satisfy certain requirements. They should be designed to allow diffusion of nutrients to the transplanted cells and guide cell organization, attachment, and migration. They also should be biodegradable and bioresorbable. In addition, scaffold materials should reduce immune response to allogenic cell.

Pore size and porosity are other important parameters. They have to allow optimum cell invasion, fibrovascular tissue and new blood vessels. The mechanical properties of the material should match that of the tissue. Mechanical properties of scaffolds during degradation and bone regeneration must be characterized. There is increasing evidence that changes in scaffold surface chemistry and topography alter cellular activity (Ishaug et al., 1997). Therefore, surfaces may need to be characterized or even altered to facilitate bone tissue regeneration.

1.3.2.1. Ceramics

Hydroxyapatite (HAP) and tricalcium phosphate (TCP) are the most widely used ceramic materials in tissue engineering of tissues and organs. There are some drawbacks of using ceramics. Ceramics are brittle and have poor tensile strength. Their use in clinical situations requiring significant torsional, impact or shear stress is limited. The rate of bioresorption of ceramics depends on their chemical composition but are generally much lower than the other types.

Hydroxyapatite is a slowly resorbing calcium phosphate ceramic. Due to the insoluble, and inert structure of crystalline hydroxyapatite, remodeling is extremely slow. Large amounts of hydroxyapatite may remain in the body for 10

years (Gazdag et al., 1995). It does not lead to immunologic reactions and was shown earlier that it was invaded by fibrovascular tissue and then converted to mature lamellar bone (Chapman et al., 1997). This newly formed bone was nearly identical to that seen in autogenous grafts. Holmes et al. (1986) also showed resorption of the surface of the hydroxyapatite implant by osteoclast-like cells. Since the structure of hydroxyapatite is inert and almost insoluble, remodeling was extremely slow. They did not observe any immunological or giant cell reaction surrounding implants. Since hydroxyapatite implants are brittle and remodel slowly, they have not been recommended for diaphyseal defects (Fleming et al., 2000). They would leave diaphyseal sites susceptible to fatigue fracture through the presence of the residual implant or to fracture at the junction between the implant and the host bone.

TCP is a calcium phosphate ceramic that is reabsorbed 10 to 20 times faster than hydroxyapatite. Since the porosity of bulk TCP implants is too low, bone ingrowth within the matrix material becomes difficult (Goldberg et al., 1991). Due to increased porosity of the matrix and the bioavailable surface, granules of TCP may be more effective than bulk TCP. Frost (1991) showed that the presence of TCP might stimulate local osteoclasts, which in turn stimulate osteoblastic activity with new bone formation. Injectable calcium phosphate cement containing α-TCP, dibasic dicalcium phosphate and tetracalcium phosphate monoxide was used by Jupiter et al. (1997). They showed that these cements are useful for treatment of distal radius fractures. In order to increase the rate of resorption of HAP, several modifications have been tested. One of them is formation of a composite of hydroxyapatite and calcium carbonate (Fleming et al., 2000). Material is almost entirely calcium carbonate that is coated with a thin layer of hydroxyapatite. Another alternative is a

composite of hydroxyapatite (30 %) and the more soluble TCP (70 %) (Buckholz, 1987, Zerwekh et al., 1992). Implantation of this material made the new bone formation more stable and longer lasting.

Calcium sulphate hemihydrate (plaster of Paris) was used by Turner et. al. (1999) as a synthetic graft material. They reported that it was absorbed by osteoclasts in several animal studies. In contrast to other ceramics, host bone formed in concentric layers around the resorbing plaster of Paris.

1.3.2.2. Reconstituted Biological Materials

1.3.2.2.1. Demineralized Bone Matrix (DBM)

Demineralized bone matrix (DBM) is a potent inducer of bone formation. It contains a bone inducing substance that causes the responding mesenchymal cells to undergo differentiation into chondroblasts, osteoblasts, and hematocytoblasts with the resultant formation of endochondral bone. DBM also retains growth factors, and noncollagenous bone proteins such as osteocalcin and osteopontin. DBM can be used alone or in combination with autogenous bone grafts or ceramics (Khan, 2000a).

Urist (1965) implanted the demineralized bone into muscle pouches in rodents and found out that it stimulates the formation of ectopic bone. Glowacki and Mulliken (1985) used DBM into craniofacial reconstruction with success. DBM was also used efficiently in osseous defects such as bone defects in children, nonunited fractures, comminuted fractures, and arthrodeses (Tiedeman et al., 1995).

Polydioxanone has been combined in semi-rigid sheet form with demineralized bone matrix (DBM) in rat calvarial defects. It functioned as a restraining agent for the particulate DBM, and provided shape control (Nichter et al., 1992).

1.3.2.2.2 Collagen

Collagen is the most abundant single protein in most vertebrates. It is the matrix on which the mineral constituents precipitate. It forms the major portion of tendons and it is an important constituent of skin. Collagen is characterized by its typical triple-helical domain. About 90% of the human collagen are the Type I found mainly in skin and bones, whereas collagen Type II is the major constituent of cartilage. Collagen contains information such as particular amino acid sequence that may facilitate cell attachment or maintenance of differentiated function. However, high rate of degradation is the major drawback of this material. In order to prevent this rapid degradation, collagen can be crosslinked or incorporated with various compounds including calcium phosphate.

A nano-HAp/collagen (nHAC) composite that mimics the natural bone both in composition and microstructure to some extent was employed as a matrix for the tissue engineering of bones (Du et al., 1999). The porous nHAC scaffold provided a microenvironment resembling that seen *in vivo*, and cells within the composite eventually acquired a tridimensional polygonal shape. In addition, new bone matrix was synthesized at the interface of bone fragments and the composite. Yaylaoğlu et al (1999) deposited HAP crystals in a collagen foam before seeding with chondrocytes. The treatment increased the stability of the foam in the *in vitro*

medium and cell proliferation was observed in the form of ECM deposition. Hsu et al. (1999) used microspheres of hydroxyapatite/reconstituted collagen as a support for osteoblast growth and concluded that these microspheres could be used as the filling material for bone defects. Cornell et al. (1991) compared Collagraft plus autogenous marrow versus cancellous iliac bone grafts in acute long bone fractures. Collagraft is a commercially synthesized composite of suspended, deantigenated bovine fibrillar collagen and porous calcium phosphate ceramic (65 % hydroxyapatite and 35 % TCP). It is non-osteoconductive and the addition of autogenous bone marrow provides osteoprogenitor stem cells. At the end of the study, they found no significant or radiographic differences. The use of Collagraft shortened operative time and avoided the operative morbidity of harvesting iliac crest bone grafts.

1.3.2.3. Synthetic Polymeric Materials

1.3.2.3.1. Synthetic Hydrogels

Mooney and Mikos (1999) have studied the potential of injectable, biodegradable hydrogels, gelatin like, water-filled polymers, for treating dental defects, such as poor bonding between teeth and the underlying bone, through guided bone regeneration. The hydrogels can be made to incorporate molecules that both modulate cellular function and induce bone formation. They provide a scaffold, on which new bone can grow and minimize the formation of scar tissue within the regenerated region. Main disadvantage of hydrogels is their lack of strong

mechanical properties. For example, fiber reinforcement of hydrogels was crucial for their use as skin substitute. Hydrogels provide a moist wound covering which help healing and also protect the wound from infection.

Hyaluronic acid is found in normal joint fluid, early fracture callus and hyaline cartilage. It is generally used in the eye to replace the vitreous humor and can also be used for intra-articular injection in the knee in early osteoarthritis. The degradation rate of hyaluronic acid can be modulated through covalent cross-linking.

Solchaga et al. (1999) used two biomaterials (HYAFF 11 and ACP) based on hyaluronic acid modified by esterification of the carboxyl group of the glucuronic acid. Those materials were tested as osteogenic or chondrogenic delivery vehicles for rabbit mesenchymal progenitor cells and compared with a well characterized porous calcium phosphate ceramic delivery vehicle. They found that the hyaluronic acid-based delivery vehicles are superior to porous calcium phosphate ceramic in terms of the number of cells loaded per unit volume of implant and HYAFF 11 sponges are superior to the ceramics with regard to the amount of bone and cartilage formed. Additionally, hyaluronic acid-based delivery vehicles have the advantage of degradation/resorption characteristics that allow complete replacement of the implant with newly formed tissue.

1.3.2.3.2. Polyurethanes

Polyurethane was used as a guided tissue regeneration application to help heal a rabbit radius defect (Nielsen et al., 1992). It was in tube form and was wrapped around the defect. Ten out of ten defects healed, compared to one out of ten

untreated controls. In this application, the tube of polymer has prevented the ingress and ingrowth of tissues different from the injured tissue during healing.

Saad et al. (1999) showed the chondrocyte and osteoblast compatibility on biodegradable polyester-urethane foam. During the degradation of this composite structure, small crystalline particles of short chain poly-((R)-3-hydroxybutyric acid) (PHB-P) and lysine methyl ester were released and osteoblasts showed only limited PHB-P phagocytosis and no signs of any cellular damage at low concentrations. At high concentrations of PHB-P the cell viability of macrophages, and to a lesser extent of osteoblasts, was affected.

1.3.2.3.3. Poly(propylene fumarate) (PPF)

The main advantage of this unsaturated polymer is its ability to cure *in vivo*, thereby facilitating the ability to fill defects of any shape or size with minimal surgical intervention. Poly(propylene fumarate) (PPF) has been incorporated into composite materials to replace trabecular bone in high local concentrations (Gerhart et al., 1988). The fumaric acid double bond of polymer chain has been used to secondarily cross-link the PPF during formulation of the composite material (Hasırcı et al., 2000). This material has demonstrated adequate mechanical properties *in vitro* to function as a temporary trabecular bone replacement (Yaszemski et al., 1996b).

Peter et al. (1997) studied a partially saturated poly(propylene fumarate) (PPF) for filling skeletal defects. The mechanical properties of the polymer were similar to that of trabecular bone. This material was also evaluated as an injectable scaffold as a composite with β-tricalcium phosphate (β-TCP) (Peter et al.,

1998). This PPF/β-TCP was evaluated both *in vitro* and *in vivo* for orthopedic applications (Peter et al., 2000, Yaszemski et al., 1995).

1.3.2.3.4 Polylactic acid (PLLA), Polyglycolic acid (PGA), and Copolymers (PLGA)

Naturally occurring hydroxy acids such as glycolic and lactic acids have been utilized to synthesize an array of useful biodegradable polymers for a variety of medical product applications including tissue engineering. Poly(L-lactic acid) (PLLA), poly(glycolic acid) (PGA), and poly(lactic-co-glycolic acid) (PLGA) are the most commonly used types. Their predominant degradation mechanism is hydrolytic. The degradation rate of these polymers is determined by the initial molecular weight, exposed surface area, pH, bond type, crystallinity, steric hindrance, and water uptake (Göpferich, 1996).

Poly(glycolic acid), poly(lactic acid) and their copolymers are the most widely used synthetic degradable polymers in medicine. There is no linear relationship between the ratio of glycolic acid to lactic acid and the physical and mechanical properties of their copolymers. PGA has the simplest structure. Since PGA is highly crystalline, it has a high melting point and low solubility in organic solvents. Due to presence of an extra methyl group in lactic acid, PLA is more hydrophobic than PGA and therefore PLA is more soluble in organic solvents than PGA. They undergo nonenzymatic hydrolysis of the polyester bond eventually resulting in either lactic or glycolic acid (Behravesh et al., 1999). Release of these degradation products can cause a decrease in the local pH and at high concentrations

these results in tissue damage. Pore sizes, porosity and degradation rates of PLGA foams can be controlled and varied by adjusting processing parameters.

The poly(α-hydroxy acid)s have a modest range of mechanical properties and a corresponding range of processing conditions. They are thermoplastic and can be formed into foams, films, tubes, and matrices using standard processing techniques as molding, extrusion, solvent or spin casting (Göpferich, 1996).

Poly(D,L-lactic-co-glycolic acid) copolymers have been widely used as drug delivery systems, sutures, temporary scaffolds for cell transplantation (Ishaug et al., 1997, Lu et al., 1998) to regenerate various tissues and as carriers for delivery of bioactive molecules (Takahata et al., 1998) since they can be easily processed into the desired configuration and their physical, chemical, mechanical and degradative properties can be engineered to fit a particular need.

Poly(α-hydroxy esters) are promising substrates for transplantation and have been extensively used in tissue engineering studies because of their biocompatibility, shown during their use as suture material and as time-release delivery systems for peptide growth factors.

The early studies with those polymers were not very satisfactory. They are well tolerated in the early phase after implantation but an inflammatory response is noted in tissues surrounding implants (Fleming et al., 2000). Bostman et al. (1990) reported adverse foreign body reaction nearly in all clinical studies with PLGA fracture fixation screws.

Among the poly(α-hydroxy esters), PLLA has the highest mechanical strength and was investigated for orthopedic applications in the form of pins, screws,

and plates (Rader et al., 1992). However, although PLLA proved to be biocompatible, there is a great concern regarding the irritancy or toxicity of degradation products that include lactic acid and undegraded PLLA particles. The amount of lactic acid released during the course of PLLA degradation is very small, but increases rapidly as PLLA is broken down to low molecular weight oligomers. This event leads to decrease in local pH, which in turn may accelerate the PLLA degradation rate and induce an inflammatory reaction. This problem may be overcome by using polydispersed PLLA though with a compromise in mechanical properties (von Recum et al., 1995). The use of polydisperse PLLA results in lactic acid production over a long period of degradation. The formation of undegraded PLLA microparticles due to the difference in degradation rates between the crystalline and amorphous regions of PLLA is known to trigger foreign body inflammatory reactions and may be to bone resorption as observed with PLLA implants.

Osteoblasts cultured on PLGA films were found to attach, proliferate, migrate and secrete collagen and alkaline phosphatase (ALPase) at rates comparable to tissue culture polystyrene (Ishaug et al., 1994). Long-term three-dimensional *in vitro* studies of porous PLGA foams demonstrated potential for bone regeneration (Ishaug et al., 1997). In an *in vivo* study, a rat nonunion defect was treated with a periosteal cell/polymer construct and a chondrocyte/polymer construct (Vacanti et al., 1995). The polymer scaffold was a nonwoven mesh of PGA fibers. The results strongly suggested that these polymer constructs had great potential in delivering bone cells to the defect site and therefore have osteoinductive potential.

Ishaug et al., (1997) demonstrated that osteoblasts on polymer films migrate from isolated osteoblast cultures and bone chips as a monolayer of cells and continue to proliferate to form multilayers. They also reported the formation of ectopic bone in rat mesentery by using PLGA foams.

1.3.2.3.5. Polycaprolactone

Poly(ε-caprolactone) (PCL) is a biodegradable and nontoxic polyester that is related to PLA and PGA with similar biocompatibility (Pulapura and Kohn, 1992). PCL is considerably less expensive than other biodegradable polyesters, such as poly(glycolide), poly(lactide), and their copolymers. However, the high crystallinity and hydrophobicity of PCL resulted in long *in vivo* degradation times ranging from 1 to 2 years (Pitt et al., 1981 and 1988). This led to heightened interest in poly-caprolactone as a long-term drug delivery (Peyman et al., 1996, Lemmouchi et al., 1998). Several approaches were used to modify the degradation properties of PCL; these strategies include the addition of catalysts (Pitt and Gu, 1987), the synthesis of copolymers (Uyama and Kobayashi, 1994), and the preparation of polymer blends (Cha and Pitt, 1990).

Lowry et al (1997) compared fixation of rabbit humeri osteotomies with polycaprolactone and stainless steel. Polycaprolactone fixation caused less stress shielding than stainless steel; nevertheless, the malunion rates reported with polycaprolactone indicated that its mechanical strength was not sufficient for load-bearing applications.

1.3.2.4. Microbial Polyesters

1.3.2.4.1. Poly(3-hydroxybutyric acid-co-3-hdroxyvaleric acid) (PHBV)

Poly(hydroxyalkonate)s (PHA) are degradable, biocompatible and thermoplastic polyesters produced by various microorganisms and also by genetically modified plants. They are intracellular storage polymers used as reserve of carbon and energy. Depending on the growth conditions, bacterial strain, and carbon source, a large variety of polymers can be obtained and their molecular weights range from tens into the hundreds of thousands.

The most extensively studied PHA is the simplest: poly(3-hydroxybutyrate) (PHB) and can be produced in high yield by fermentation of a variety of bacterial strains. Its copolymers with varying ratios of hydroxyvalerate (HV) are the most widely used members. The copolymers of hydroxybutyrate with hydroxyvaleric acid are less crystalline, more flexible and more readily processable than PHB itself (Mitomo et al., 1987) (Gassner and Owen, 1996). Their various properties such as natural origin, biodegradability, biocompatibility, non-toxic, streospecificity, piezoelectricity, optical activity, and thermoplasticity make them suitable for a variety of applications in medicine and industry as presented in Table 1.1 (Pouton and Akhtar, 1996).

Table 1.1. Applications of PHAs

Medical Applications:
* Surgical pins, sutures, staples, and swabs
* Wound dressings
* Blood vessel replacements
* Bone replacements and plates
* Stimulation of bone growth by piezoelectricity properties
* Biodegradable carriers for long term dosage of drugs and medicines
*Tissue engineering
Industrial Applications
*Biodegradable carriers for long term dosage of herbicides, fungicides, insecticides or fertilizers
*Packaging containers, bottles, wrappings, bags and films
*Disposable items such as hygiene products

Poly(β-hydroxybutyrate) (PHB) was first discovered in *Bacillus megaterium* in 1925 by Lemoigne at the Pasteur Institute in Paris. It has been clear that PHB is not just an inert storage polymer, confined to certain bacteria, but interactive, solvating biopolymer involved in important physiological functions.

Low molecular weight PHB complexed to other macromolecules (c-PHB) is widely distributed in biological cells of representative organisms of nearly all phylla. Complexation modifies the physical and chemical properties of c-PHB, allowing it to pass through both hydrophilic and hydrophobic barriers of the cell (Reusch, 1995). Muller and Seebach (1993) suggested that PHAs might be the fifth class of physiologically important organic biopolymers, joining the proteins, polynucleotides, polysaccharides and polyisoprenoids.

The biocompatibility of PHB and PHBV has been studied by a number of different research groups. PHB has been found to have low toxicity, in part due to the fact that it degrades *in vivo* to D-3-hydroxybutyrate, a normal constituent of human blood (Reusch, 1995). The general structure for PHBV is given below:

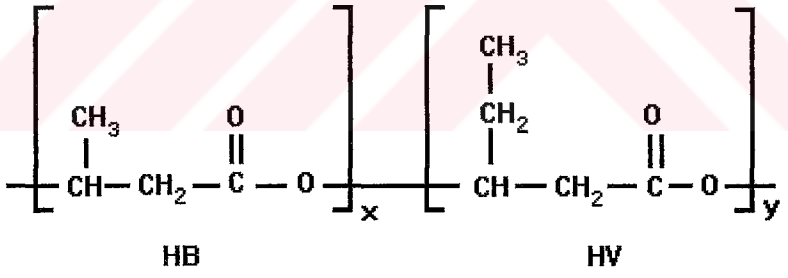

Figure 1.5. The chemical structure of P(HB-HV) copolymers

Poly(3-hdroxybutyric acid-co-3-hydroxyvaleric acid), PHBV is an optically active polyester consisting of D-β-hydroxybutyric acid (PHB) and D-β-hydroxyvaleric acid as a repeating unit. PHB is produced by microorganisms and it is also a normal constituent of human blood. It is produced by various strains of

microorganisms such as *Bacillus megaterium*, glucose utilizing mutant of *Alcaligenes eutrophus* etc., soil bacteria, estuarine microflora, blue green algae, microbiologically treated sewage. In microorganisms, PHB serves as an intracellular energy and carbon storage product in much the same way as glycogen in mammalian tissue. It is also thought to have minor roles in cellular functions such as sporulation, encystment, and gene expression. The polymer accumulates in discrete membrane bound granules in the bacterial cells from which it can be extracted directly with organic solvents such as chloroform or by membrane rupturing techniques. It is safe, nontoxic, biocompatible, biodegradable, easily and reproducibly processable. The related copolymers of PHB with β-hydroxyvaleric acid (PHBV) emerge as a new generation of PHB-based materials with more adjustable properties depending upon copolymer composition. Degradation rate of PHBV can easily be adjusted by changing the copolymer composition. PHB and PHBV matrices lose mass very slowly when compared to bulk-degrading poly(lactide-glycolide) systems. Poly(hydroxybutyric acid-co-valeric acid) are semicrystalline polymers that have high degrees of crystallinity (60-80%). Crystallinity influences polymer properties such as rate and mechanism of degradation, drug compatibility and drug release. PHBV are also biocompatible (Koosha et al., 1989; Pouton and Akhtar, 1996). Besides, they are known to exhibit piezoelectricity (Fukada and Ando, 1986). Since electrical stimulation is thought to promote bone healing and repair. These polymers have been suggested for use as bone pins and plates.

Rivard et al. (1996) demonstrated that PHBV (9%) sustained fibroblast cell proliferation rate similar to that observed in collagen sponges for up to at least 35 days. On the other hand, the PHBV materials maintained their integrity during the

culture period while the collagen foams contracted substantialy. Moreover, the total protein production after 4 weeks in culture was found to be twice as high in the PHBV foam than in the collagen foam. Porous PHBV materials appear to be adequate polymeric substrates for cell cultures.

All polymers were well tolerated by the tissue when implanted subcutaneously. No acute inflammation, abscess formation or tissue necrosis was observed in tissues adjacent to the implanted materials, which were either in the form of nonporous discs or cylinders. Mononuclear macrophages, proliferating fibroblasts and mature vascularized fibrous capsules were typical of the tissue response (Muller and Seebach, 1993, Gogolewski et al., 1993). When PHBV was implanted in rabbit tibia as a carrier of antibiotics cefoperazone and sulbactam, there were no significant symptoms of chronic inflammation or toxicity as judged by histology, SEM, microbiology and X-ray studies (Gürsel et al., 2001).

The properties can be optimized by blending or by selecting the appropriate PHA, therefore, provide a wealth of options for cell carriers which could be tailored for specific engineering applications. Degradation rate of PHBV influences the mechanical and physical properties of its constructs. It is also influential on its biocompatibility and therefore is very critical. It can easily be adjusted by changing the copolymer composition or by blending with other compounds. PHB and PHBV matrices lose mass very slowly when compared to bulk-degrading poly(lactide-co-glycolide) systems. PHBV have high degrees of crystallinity (60-80%) and these influence polymer properties such as rate and mode of degradation, drug compatibility and drug release.

Hydroxyapatite (HA) and other fillers were used to modify the mechanical properties of the polymer for certain medical applications. Composites of PHBV and hydroxyapatite with partial biodegradability and high mechanical strength and osteoconductivity were found to be suitable for fracture fixation (Galego et al., 2000). A composite of PHB polymer reinforced with synthetic hydroxyapatite particles was tried as a bone analogue and new bone growth at the interface of implantation site was observed after six months (Luklinska and Bonfield, 1997).

1.3.3. Bone Growth Factors

Bioactive agents are essential in the success of tissue engineered constructs and therefore various types are used and a number of delivery approaches have been developed.

1.3.3.1. Types of Bone Growth Factors

Growth factors when combined with implants would yield a much faster and better tissue repair. Some growth factors play a critical role in bone healing and regeneration. These tissue specific polypeptides act as local regulators of cellular activity. They bind to cell-surface transmembrane receptors on the target cell and the intracellular domain is stimulated. This event usually causes an activation of specific protein kinases leading to activation of transcription of a gene into mRNA and translation of proteins for use intracellularly or extracellularly (Solheim, 1998). These growth-promoting factors include BMPs, insulin-like growth factors, (IGF)

transforming growth factor-β (TGF-β), fibroblast growth factors (FGF), and platelet derived growth factors (PDGF).

1.3.3.1.1. BMPs

BMPs appear to be the most promising, low molecular weight peptides that initiate bone formation by recruiting and stimulating local progenitor cells of osteoblast lineage and by enhancing bone collagen synthesis (Khan et al., 2000b). They belong to an expanding TGF-β super family. They play an important role in the formation and maturation of skeletal tissues. They can be extracted from bone, dentine, osteosarcomata or metastases of prostate cancer. More than 24 have been identified. BMP-2, BMP-4, and BMP-7 are the most studied and osteoinductive. They stimulate alkaline phosphatase activity and collagen synthesis by osteoblastic cells *in vitro*. BMP-7 (OP-1) promotes chondroblastic and osteoblastic differentiation and formation of mineralized matrix by osteoblasts.

1.3.3.1.2. Transforming Growth Factor-β (TGF-β)

Transforming growth factor-β, a chemotactic mediator for fibroblasts and macrophages, blocks plasminogen inhibitor, increases angiogenesis, and stimulates collagen synthesis, mesenchymal cell growth, differentiation, and bone repair. It inhibits procollagenase and epithelial expansion but increases the osteoinductive activities of the BMPs. Moreover, TGF-β regulates the proliferation of chondrocytes and synthesis of a cartilage matrix. There are three isoforms of

TGF-β. Type 1 is stored in platelet alpha granules and plays a crucial role in fracture repair.

1.3.3.1.3. Platelet Derived Growth Factor (PDGF)

Platelet derived growth factor is synthesized by platelets, macrophages, monocytes and endothelial cells. It increases DNA synthesis, cell replication, production of collagen, and noncollagenous proteins (Canalis 1988). PDGF play a role in fracture repair and osteoclast activation.

1.3.3.1.4. Insulin-like Growth Factor (IGF)

Insulin-like growth factor promotes cellular proliferation and matrix synthesis by osteoblasts and chondroblasts (Khan et al., 2000b). IGF-II is the most abundant isomer in human bone cells.

1.3.3.1.5. Fibroblast Growth Factors (FGF)

Fibroblast growth factors act on stem and differentiated cells, causing changes in migration, proliferation, differentiation, morphology, and function. They are mitogenic factors that are produced in early phase of fracture repair and localized in the bone matrix. Acidic and basic fibroblast growth factors induce and inhibit bone repair, depending on the applied dose.

1.3.3.1.6. Other Bioactive Agents

The growth rate and viability of the bone cells can be improved by incorporating bioactive agents such as ascorbic acid, β-glycerophosphate, and dexamethasone. Since culture conditions have been shown to affect osteoblast activity (Maniatopoulos et al., 1988; Coelho and Fernandes, 2000), some medium supplements such as L-ascorbic acid, β-glycerophosphate and dexamethasone were used for osteoblast growth. Osteoblasts obtained from fetal calvaria secreted mineralized matrix when L-ascorbic acid and β-glycerophosphate were added to the medium. L-ascorbic acid is an enzyme cofactor and antioxidant that stimulates the transcription, translation and posttranslational processing of collagen in connective tissue cells. In culture of bone-derived cells, ascorbate stimulates osteoblastic differentiation, synthesis and deposition of collagen and mineralization. Ascorbate influences the differentiation of preosteoblasts and is required for the synthesis of osteoid by mature osteoblasts. Ascorbate and β-glycerophosphate are the inducers of osteogenic differentiation. In the presence of β-glycerophosphate, bone matrix deposition is induced and increased with time in culture. Dexamethasone, a glucocorticoid, increased the number of collagenous mineralized nodules found in calvaria culture and extended the days that nodules formed in culture. Stromal cells obtained from bone marrow also secreted matrix with collagenous, mineralized nodules but only when the medium supplemented with both β-glycerophosphate and dexamethasone. Differentiated cultured bone cells provide an essential tool for investigating biodegradable scaffolds for bone tissue regeneration. In addition,

enhancement of osteoblast differentiation on scaffolds prior to transplantation may improve effectiveness of this type of bone regeneration therapy. For those reasons differentiation of mesenchymal cells play a very important role.

1.3.3.2. Bone Growth Factor Delivery

Bone growth factors play an important role in bone tissue regeneration or repair. However, most of them have short half-lives after intravenous injection (Saltzman, 1996). Therefore, their biological activity lasts only a few minutes in the circulation and repeated injection is required to obtain sustained blood levels. These molecules are extremely potent and are large, therefore, they penetrate the tissue barriers very slowly but their systemic administration can lead to toxicity. In order to solve these problems, new delivery methods are required for growth factors. Polymers can be designed so that scaffold materials constructed using them provide both structural and controlled-release functions.

Polymeric controlled delivery has been carried out by a number of researchers. BMP was delivered to a segmental rabbit tibial defect via a polymer containing PLLA, PEG, and PLGA (Miyamoto and Takaoka, 1993). The researchers reported a complete restoration of the defect in 12 weeks. Yasko et al. (1992) used rat DBM as a carrier and delivered BMP-2 in a rat femoral defect. They reported complete healing of the defects. BMP was delivered to treat non-unions in a PLLA-PLGA delivery system (Johnson et al., 1990). All patients healed within 5 months after the treatment. BMPs were also carried with a PLGA-TCP composite (Desilets et al., 1990), collagen (Gao et al., 1993), plaster of Paris (Yamazaki et al., 1988), and

hydroxy apatite impregnated with collagen (Takaoka etal., 1988). These systems all resulted in the formation of new bone in heterotopic sites, and reported higher bone formation with increasing BMP doses. The addition of bioactive molecule was shown to induce bone growth to occur faster and in greater mass.

Liebergall et al. (1994) incubated cells in TGF-β1 and delivered by ceramic carriers to the defect site. They observed an increase in bone growth. Sumner et al. (1995) used titanium rods plasma-flame sprayed with HA and TCP for canine bilateral implantation. They treated the implants with TGF-β1 and observed increase in bone growth.

Bovine collagen was used as a TGF-β vehicle becuse it is highly purified, hypoallergenic, and can form a viscous suspension that can easily be applied to the cut edges of an incision (Beck et al., 1993). They reported slow release and prolonged local exposure to TGF-β. Strates et al. (1992) observed large amount of bone formation in a non-union study in dogs by using TGF-β adsorbed on resorbable microcrystals of hydroxyapatite.

An application of human recombinant TGF-β1 in a 3% methylcellulose gel to skull defects created in rabbits induced a dose dependent increase in intramembranous bone formation (Beck et al., 1991). TGF-β1 delivery was also achieved by using PLGA and DBM (Gombotz etal., 1993). Most of the TGF-β1 released from the delivery system retained its bioactivity and the devices were sufficiently porous to allow bone ingrowth.

1.4. The Approach in This Study

Most commonly used matrix materials in bone tissue engineering are synthetic polymers because of their versatility. In this study two matrices of natural origin were used. Rapid degradation of collagen was prevented through incorporation of calcium phosphate into its structure. PHBV is a very promising polymeric matrix material. Its degradation rate is slower than those of other synthetic or natural polymer systems. Besides, it is possible to add side groups and carry out surface modifications such as rf-oxygen plasma treatments that make the polymer surface more hydrophilic. This strategy was expected to offer many of the advantages of bone grafting while avoiding the complications of immune rejection, donor site morbidity, and limited availability. Thus it would be possible to offer an effective treatment for cases of bone tissue or function loss.

The ultimate aim was to obtain optimum osteoblast growth on scaffolds via modification of matrix structures. For that reason, the porosity and the surface chemistry of the matrix materials were changed. Both matrix degradability and *in vitro* cell proliferation and differentiation were studied via biochemical, immunohistochemical and microscopic methods.

CHAPTER 2

MATERIALS AND METHODS

2.1. Materials

Poly(3-hydroxybutyrate-co-3-hydroxyvalerate) (PHBV8 containing 8% by mole of hydroxyvalerate) was purchased from Aldrich (Chem. Co., Milwaukee, MI, USA). Chloroform, diethyl ether and dichloromethane were of analytical grade and purchased from E. Merck AG (Germany). Sucrose, sodium chloride, Tris, sodium azide, calcium chloride and sodium ammonium hydrogen phosphate ($NaNH_4HPO_4.4H_2O$) were products of E. Merck AG (Germany). Gelfix® was obtained from Abdi İbrahim (Turkey). Formaldehyde, sodium dihydrogen phosphate, glutaraldehyde, sodium cacodylate, L-ascorbic acid, β-glycerophosphate, dexamethasone, alkaline phosphatase kit (Procedure No. ALP-10), Anti Integrin IgG Ab, and Dulbecco's Minimal Medium (DMEM) (high glucose 4.5 g/L and low glucose 1 g/L) were purchased from Sigma Chemical Company (USA). Trypsin-EDTA (0.05 %) and fetal calf serum (FCS) were products of Biochrom KG

(Germany). The reagents and polystyrene culture dishes for cell culture studies were all cell culture tested. MTS kit was obtained from Promega (USA).

2.2. Methods

2.2.1. Preparation of Poly(3-hydroxybutyric acid-co-3-hydroxyvaleric acid) (PHBV8) Foams

2.2.1.1. Unmodified PHBV8 Foams

Different concentrations (4, 6, or 8 %, w/w) of poly(3-hydroxybutyrate-co-3-hydroxyvalerate) containing 8% by mole of hydroxyvalerate (PHBV8) were prepared in chloroform:dichloromethane (1:2, v/v). PHBV8 solutions were poured onto the Petri plates and air dried. They were frozen at -70 °C and lyophilized in a freeze dryer (Labconco Freeze Dry (Missouri, USA), Model 78680). Matrices were cut into disks of 7 mm diameter and 1.9 mm thick and sterilized by exposure to gamma radiation (25 kGy).

2.2.1.2. Sodium chloride loaded PHBV8 Foams

Biodegradable PHBV8 foams were prepared by solute leaching method. Crystalline sodium chloride (< 150 μm) (55 g) was placed in a glass Petri dish and PHBV8 (6%, w/w) solution in chloroform was poured onto the crystals until they were submerged. It was air-dried and dialyzed against distilled water for 2 days

to remove all soluble crystals. It was, then, frozen at -70 °C and lyophilized in a freeze dryer (Labconco Freeze Dry (Missouri, USA), Model 78680). Matrix was cut into disks of 7 mm diameter and 1.9 mm thick and sterilized by exposure to gamma radiation (25 kGy).

2.2.1.3. Sucrose loaded PHBV8 Foams

In order to obtain a highly porous matrix and also to create uniform pore sizes, sieved sucrose crystals (75-300 μm or 300-500 μm) were used. Sucrose crystals (50 g) were placed in a glass Petri dish. Chloroform solutions of PHBV8 with different concentrations (4, 6, or 8 %, w/w) were prepared as described in Section 2.2.1.1 and the solutions were poured onto the sucrose crystals until they were submerged. They were then air-dried and the resultant foams were dialyzed against distilled water for 2 days to remove all the sucrose, resulting in porous PHBV8 matrices. They were frozen at -70 °C and lyophilized in a freeze dryer (Labconco Freeze Dry (Missouri, USA), Model 78680). Matrices were cut into disks of 7 mm diameter and 1.9 mm thick and sterilized by exposure to gamma radiation (25 kGy).

2.2.1.4. Oxygen Plasma Treatment of PHBV8 Foams

PHBV8 foams (unloaded and sucrose loaded) were prepared from chloroform:dichloromethane (1:2, v/v) solutions with different concentrations (4, 6, or 8 %, w/w) as reported in Sections 2.2.1.1 and 2.2.1.3 The surfaces of these

PHBV8 matrices were then treated with oxygen rf-plasma (Advanced Plasma System, Inc., USA) at 50 W for 10 min, 50 W for 20 min, 100 W for 10 min, and 100 W for 20 min, in order to make the surfaces more hydrophilic.

2.2.2. Preparation of Collagen (Gelfix®-Calcium Phosphate) Foams

Calcium phosphate formation on Gelfix® (Abdi İbrahim, Turkey, lyophilized collagen foam (50x50x50 mm^3) was done according to Yaylaoğlu et al. (1999). Gelfix® was soaked overnight in a phosphorous solution in Tris buffer (100 mM, pH 7.4, 50 mM Tris, 1 % NaN_3). The foam was removed, immersed overnight in a calcium solution in Tris buffer (100 mM, pH 7.4, 50 mM Tris, 1 % NaN_3) and washed with distilled water for 2 hours. This calcium phosphate formation procedure was then repeated. The foam was frozen at -70 °C and lyophilized in a freeze dryer (Labconco Freeze Dry (Missouri, USA), Model 78680). It was then cut into disks of 7 mm diameter and 1.9 mm thick and sterilized by exposure to gamma radiation (25 kGy).

2.2.3. Characterization of Foams

2.2.3.1. SEM

Surfaces of the untreated and unloaded PHBV8 (4, 6, and 8 %, w/w), sucrose loaded PHBV8 (4, 6, and 8 %, w/w), oxygen plasma treated PHBV8 (4, 6, and 8 %, w/w), Gelfix® (lyophilized collagen foam) and Gelfix®-calcium phosphate

foams were all coated with gold and SEM was carried out in a JEOL (Japan), Model JSM 6400 to observe the surface characteristics, pore sizes and the pore distribution of the matrix materials.

2.2.3.2. SEM Coupled with Energy Dispersive Spectra (SEM-EDS)

The ratio of calcium to phosphate in the Gelfix®-calcium phosphate matrix was determined by the EDS capability of the SEM (NORAN (USA), series 2). The samples were coated with gold under vacuum and ED spectra was obtained.

2.2.3.3. Porosity Analysis

Average pore size and the pore distribution of the untreated and unloaded PHBV8 (4, 6, and 8 %, w/w), untreated and large sucrose loaded (300-500 μm) PHBV8 (6 %, w/w), oxygen plasma treated PHBV8 6% (100 W 20 min), untreated and small sucrose loaded (75-300 μm) PHBV8 6%, untreated and sodium chloride loaded PHBV8 6%, Gelfix®, and Gelfix®-calcium phosphate foams were examined using the Scion Image Analysis Program (National Institudes of Health (NIH) image) which is a public domain image processing and analysis program for the Macintosh.

2.2.3.4. Void Volume and Density Calculations

Volume of pores inside the polymers was determined to find out the volume available for cell loading. First, dry weights of the untreated and large size

sucrose loaded (300-500 μm) PHBV8 (4, 6, and 8 %,w/w), oxygen plasma treated PHBV8 6% (100 W 20 min), untreated and small size sucrose loaded (75-300 μm) PHBV8 6%, untreated, and sodium chloride loaded PHBV8 6%, Gelfix® and Gelfix®-calcium phosphate foams were recorded. Then, they were immersed into water and vacuum was applied to achieve penetration of water inside the pores. Finally, wet weights of the foams were recorded. Foam thicknesses were measured using a micrometer (Erste Qualitat, Germany). Volume of the pores was calculated.

Foam density was also determined by pycnometry. Above mentioned samples and empty pycnometer were weighed. Pycnometer was weighed again after completely filling with distilled water. Then, the foam was put into the pycnometer before completely filling with water, the pycnometer was then filled to the limit, and weighed again. The addition of foam displaced equal volume of water. The density of the foam was calculated from these data. However, during this process some water was adsorbed onto the foam due to its porous structure and the capillary action. Therefore, the foam was weighed again after removal from the pycnometer to compensate for this error. The method of calculation is presented in Appendix A.

2.2.3.5. Water Contact Angle Measurement

PHBV8 and Gelfix® foams were prepared as described above. The wettability of the matrices was assesed by sessile drop method using Cam-Micro (Tantec Inc., USA). A droplet of water was put onto the foams and contact angles were studied to observe the degree of hydrophilicity.

2.2.3.6. Degradation of PHBV8 and its Quantification via pH Changes and Gravimetry

For the degradation study, unloaded PHBV8 (4, 6 and 8 %, w/w), and sucrose loaded PHBV8 foams were weighed. The disks were put into 50 mL Corning flasks containing phosphate buffer (20 mL, pH 7.4, 10 mM, 0.09% sodium azide) and incubated at 37 °C for 0.5, 1, 2, 4, and 6 months. Samples of solution from each foam were collected at different time points. At the end of the period, the disks were freeze-dried for 8 h and weighed. At the same time, the pH in the supernatant (phosphate buffer) was recorded. All measurements were expressed as means ± standard deviation (sd) relative to the initial values.

2.2.4. *In Vitro* Osteoblast-Biomaterial Interaction Studies

2.2.4.1. Isolation of Osteoblasts

Stromal osteoblastic cells were obtained from the marrrow of young adult male (6-weeks old, 150-170 g) Wistar rats. Following euthanasia by diethyl ether inhalation, femora were aseptically excised, cleaned off soft tissue, and washed in Dulbecco's Modified Eagle medium (DMEM) containing 1000 units/mL penicillin and 1000 units/mL streptomycin. The metaphyseal ends then were cut off and the marrow flushed from the midshaft with 5 mL of primary media (DMEM containing 20% fetal bovine serum (FBS) and 100 units/mL penicillin and 100 units/mL

streptomycin) using a syringe equipped with a 22-gauge needle and collected in a sterile Petri dish. Cell clumps were broken by repeatedly pipetting the cell suspension. The cells then were centrifuged at 400 g for 10 min. The resulting cell pellets were resuspended in 12 mL of primary media and plated in T-75 flasks (cells from two femura per flask). They were incubated in CO_2 incubator for 4 days.

2.2.4.2. Osteoblast Culture

After 4 days of incubation, hematopoietic cells and other unattached cells were removed from the flasks by repeated washes with PBS. Then, 10 mL complete media containing DMEM supplemented with 20% FBS, 100 units/mL penicillin, 100 units/mL streptomycin, 10 mM β-glycerophosphate, 50 μg/mL L-ascorbic acid and 10 nM dexamethasone were added to promote the osteoblastic phenotype of marrow stromal cells. Complete medium was changed every other day.

2.2.4.3. Osteoblast Characterization

2.2.4.3.1. Microscopic Evaluation (Light Microscopy)

Osteoblasts, cultured on TCPs, were visualized under the inverted phase contrast microscope (Olympus MO81, Japan) after the first passage. Fujichrome 200 ASA film and B (blue) filter mounted on an Olympus microscope were used to obtain the micrographs.

2.2.4.3.2. Determination of Alkaline Phosphatase by UV Spectroscopy

Production of alkaline phosphatase (ALP) was measured spectroscopically. 2-D osteoblast cultures of second, third and fourth passages in T-75 flasks were washed with PBS and harvested. They were frozen (at – 80 °C) and thawed three more times. Protein concentrations were determined with Lowry method using bovine serum albumin as a standard. Results were expressed as μg protein/cm^2. Both sets of samples were sonicated for 4 min at 110 watts on ice. 20 μL from each sample was added to 1 mL of p-nitrophenyl phosphate solution (16 mmol/L) at 30 °C and maintained for 2 min. p-Nitrophenol was produced in the presence of alkaline phosphatase and absorbance was measured with a UV Visible spectrophotometer (Shimadzu (Japan), Model 2100S) at 405 nm after 1 and 2 min. The slope of the absorbance vs time plot was used to calculate the alkaline phosphatase activity.

2.2.4.3.3. Determination of Alkaline Phosphatase by Electrophoresis

Same samples were used as indicated in ALP spectrophotometric assay (Section 2.2.4.3.2). Two samples, fibroblast cell and human serum, were used as controls. 20 μg sample was applied to an agarose gel (SEBIA Hydragel ISO-PAL (SD), Germany) from each sample and ALP electrophoresis was carried out (100 Volts for 45 min). Then, the gel was incubated with substrate solvent at 37°C for 50 min, washed with distilled water and dried for 10 min.

2.2.4.3.4. Determination of Osteocalcin

Same samples were used as indicated in ALP spectrophotometric assay (Section 2.2.4.3.2). Amount of osteocalcin was detected by using Novocalcin® (96 assay for intact osteocalcin) kit (Metra Biosystem Inc., CA, USA). Osteocalcin standards for calibration curve and 10 µL sample were put into 96 well plate. They were incubated with anti osteocalcin and enzyme conjugate for 2 h, respectively. Absorbance was read at 405 nm. Amount of osteocalcin was detected by Scanning autoreader and microplate workstation (Ceres (USA), Model 900).

2.2.4.3.5. Cell Growth Kinetics

Osteoblasts prepared as in Sections 2.2.4.1 and 2.2.4.2 and seeded onto T-75 flasks were trypsinized and counted. Cell suspensions were diluted to have $1x10^4$, and $3x10^4$ cells/mL per 20 mL medium. They were seeded in triplicates into 24 well plate, with 1 mL/well. Plate was incubated at 37 °C in a CO_2 incubator. After 12 h, the plate was removed and the cells were counted. It was returned to the incubator as soon as cell samples in trypsin were removed. Sampling was repeated at 12 h, 24 h, 48 h, 72 h, 96 h, 120 h, 144 h, and 168 h. Medium was changed every other day. This test was carried out three times.

2.2.4.3.6. Western Blot for Integrin

2-D osteoblast culture of third passage in two T-75 flasks was scraped in to the its own medium after 21 days of incubation and centrifuged at 1200 rpm for 10 minutes at 4°C. The cell pellet was then washed twice using ice-cold PBS with protease inhibitors (1mM EDTA and 1 mM PMSF) without phenol red. The resulting pellet was weighed and resuspended in same PBS as to be 40 % (w/v) of the final volume. Following two cycles of freezing and thawing at -80°C, 40 µL cell suspension was boiled in reducing sample buffer containing Tris base, SDS, Glycerol, Glycine and β-Mercaptoethanol for 5 min. Proteins were separated in 10 % SDS-Polyacrylamide gel and transferred to polyvinilidine difluoride membrane. The membrane was blocked in TBS containing 3 % non-fat milk powder, 1 % Horse Serum and 0.05 % Tween 20 for 3 hours. After excessive washings in TBS-T, the blot was incubated with primary antibody (anti-β1 integrin MAb) overnight at room temperature. After series of washing, it was incubated with secondary antibody (anti-mouse IgG labelled with Biotyn) for two hours at room temperature. Then, the membrane was washed again and incubated with streptoavidin-biotyn complex labelled with HRPO. Bands were visualized using 4-chloronaphtol.

2.2.4.3.7. Determination of Cell Viability by Cell Titer 96^{TM} Nonradioactivity Cell Proliferation Assay (MTS Assay)

2-D osteoblast cultures were trypsinized and counted. Different concentrations of the osteoblast cells ($1x10^4$, $2.5x10^4$, $5x10^4$, $10x10^4$, $15x10^4$, $20x10^4$, $30x10^4$, $40x10^4$, $50x10^4$) were seeded on 96 well Elisa plates and incubated for 6h at 37 °C in a CO_2 incubator. MTS/PMS reagent (100 µL) was added to each well of the 96 well plate which was then incubated for 135 min at 37 °C in a CO_2 incubator (SANYO (German), Model MCO 175). Absorbance was determined at 490 nm using an Elisa Plate Reader (Molecular Devices (USA), Model Maxline) and a calibration curve using different concentrations of osteoblast cells was constructed. The calibration curve was then used in the determination of the cell concentration inside the matrices.

2.2.4.4. Seeding of Osteoblasts on Polymeric Foams or Films

When confluent monolayers was reached (yielding approximately $2x10^6$ cells/femur) the cells were enzymatically lifted from the flask using a 625 µg/mL solution of trypsin. The cells were concentrated by centrifugation at 400 g for 10 min and resuspended in 5 mL of complete media. Cells were counted by Trypan Blue staining and diluted to $1.5x10^5$ or $5x10^5$ cells/mL in complete media. Aliquots of 20 µL of cell suspension was seeded onto the top of prewetted matrices placed in the wells of 24-well plate. The matrices were left undisturbed in an

incubator for 6 h to allow the cells to attach to the matrix. Then, 1 mL of complete medium was added to each well. Medium was changed every other day.

2.2.4.4.1. Determination of Osteoblast Growth on Polymeric Films

PHBV8 films prepared by solvent evaporation of chloroform solutions were sterilized with gamma radiation and put into 24 well plates. They were seeded with cells of concentrations of $1x10^4$ and $10x10^4$ cells/mL and incubated for 7 days at 37 °C in a CO_2 incubator. At the end of 7 days, Cell Titer 96™ Nonradioactivity Cell Proliferation Assay (MTS Assay) was applied and cell growth on the PHBV8 films was observed.

2.2.4.4.2. Determination of Osteoblast Growth on Polymeric Foams with Different Pore Sizes

PHBV8 (6 and 8 %, w/w) foams were prepared as described in Section 2.2.1.3. Foams were sterilized with gamma radiation and put into a 24 well plate. Osteoblast seeded foams ($1x10^5$, $5x10^5$, $10x10^5$ cells/mL) were incubated for 7 days in CO_2 incubator (SANYO (Germany), Model MCO 175). Untreated PHBV8 was used in this experiment as a control. MTS/PMS reagent (100 µL) was added to each well of the 24 well plate and incubated for 135 min at 37 °C in a CO_2 incubator (SANYO (Germany), Model MCO 175). Absorbance was determined at 490 nm using an Elisa Plate Reader (Molecular Devices (USA), Model Maxline).

2.2.4.4.3. Determination of Osteoblast Growth on Polymeric Foams with Different Surface Treatments

PHBV8 (6 and 8 %, w/w) foams were prepared as described in Section 2.2.1.3. They also were treated with oxygen plasma (100 W 10 min). Foams were sterilized with gamma radiation and put into a 24 well plate. Osteoblast seeded foams ($1x10^5$, $5x10^5$, $10x10^5$ cells/mL) were incubated for 7 days in CO_2 incubator (SANYO (Germany), Model MCO 175). Untreated PHBV8 was used in this experiment as a control. MTS/PMS reagent (100 µL) was added to each well of the 24 well plate and incubated for 135 min at 37 °C in a CO_2 incubator (SANYO (Germany), Model MCO 175). Absorbance was determined at 490 nm using an Elisa Plate Reader (Molecular Devices (USA), Model Maxline).

In order to study the effect of extent of oxygen plasma modification of the foams on osteoblast growth inside the matrices, PHBV8 foams were treated with rf-oxygen plasma (50 W 10 min, 50 W 20 min, 100 W 10 min and 100 W 20 min) as described in Section 2.2.1.4. Foams were sterilized with gamma radiation and put into a 24 well plate. Osteoblast seeded foams ($2.5x10^5$ cells/mL) were incubated for 7 days in CO_2 incubator. MTS/PMS reagent (100 µL) was added to each well of the 24 well plate and incubated for 135 min at 37 °C in a CO_2 incubator. Absorbance was determined at 490 nm using an Elisa Plate Reader.

2.2.4.4.4. Determination of Osteoblast Growth on Polymeric Foams

PHBV8 and calcium phosphate loaded Gelfix foams were prepared as described in Sections 2.2.1.3, 2.2.1.4 and 2.2.2. Foams were sterilized with gamma radiation and put into a 24 well plate. Osteoblast seeded foams ($1.5x10^5$ cells/mL) were incubated for 21 and 29 days for PHBV8 and 7 days for Gelfix foams in a CO_2 incubator (SANYO (Germany), Model MCO 175). Cell Titer 96^{TM} Nonradioactivity Cell Proliferation assay was used to determine the cell density inside the polymer matrices. MTS/PMS reagent (100 μL) was added to each well of the 24 well plate and incubated for 135 min at 37 °C in a CO_2 incubator (SANYO (Germany), Model MCO 175). Absorbance was determined at 490 nm using an Elisa Plate Reader (Molecular Devices (USA), Model Maxline). All experiments were performed thrice.

2.2.4.4.5. Determination of Alkaline Phosphatase on Polymeric Foams

For the determination of the effect of the cell-substrate interaction on the production of alkaline phosphatase by cultured cells, cells ($1.5x10^5$ cells/polymer scaffold) were cultured for 21 and 29 days on a polymer scaffold. At each time point, the medium was removed from the wells and foams were washed three times with PBS. Then, they were freezed and thawed three times. Upon thawing, the foams were homogenized with 1 mL Tris buffer (1M, pH 8.0) and sonicated for 5 min on ice. Protein concentrations were determined with Lowry method using bovine serum albumin as a standard. Results were expressed as μg protein/cm^2 of polymer scaffold.

A volume of 20 µL of each sample was added to 1 mL of p-nitrophenyl phosphate solution (16 mmol/L) at 30 °C and maintained for 2 min. p-Nitrophenol was produced in the presence of alkaline phosphatase and was measured with a UV Visible spectrophotometer (Shimadzu (Japan), Model 2100S) at 405 nm. The absorbance was measured at 1 and 2 min and the slope of absorbance vs time plot was used to calculate the alkaline phosphatase activity. This experiment was performed in duplicate.

2.2.4.4.6. Determination of Osteocalcin on Polymeric Foams

Same samples as described in Section 2.2.4.4.5 were used in the osteocalcin study. Amount of osteocalcin was detected by using Novocalcin® (96 assay for intact osteocalcin) kit (Metra Biosystem Inc., CA, USA). Osteocalcin standards for calibration curve and 10 µL sample were put into 96 well plate. They were incubated with anti osteocalcin and enzyme conjugate for 2 h, respectively. Absorbance was read at 405 nm. Amount of osteocalcin was detected by Scanning autoreader and microplate workstation (Ceres (USA), Model 900). Experiment was performed in duplicate.

2.2.4.4.7. Determination of Mineralization (Histological Staining)

Histological staining of PHBV8 and Gelfix foams was carried out for visualization of cells and demonstration of tissue formation. Osteoblast-foam constructs were prepared for both light microscopy on plastic embedded semi-thin

sections and for acid phosphatase (ACP) enzyme histochemistry on frozen sections after 7 days for Gelfix and, 21 and 29 days for PHBV8 in culture.

For light microscopy on plastic embedded semi-thin sections, polymer-cell samples were fixed in 2.5 % glutaraldehyde (in 0.1 M sodium cacodylate buffer, pH 7.4) for 2 h. They were washed with sodium cacodylate buffer (0.1 M, pH 7.4) and postfixed in 1 % OsO_4 (in the same buffer) for 1.5 h at RT. They were then processed in a graded series of ethanol and placed in flat molds to embed in resin (Araldite C4212). They were cut into 1-3 μm thick semi-thin sections and stained with methylene blue-azur II.

For ACP staining, polymer-cell samples were immediately frozen in liquid nitrogen at the end of each incubation period (21 and 29 days) and were stored at –30 °C until further processing. The 10 μm thick cryostat sections were obtained on gelatin coated slides and kept in humidity-free containers at RT. Then, ACP activity of the samples was detected by using enzyme histochemistry. Naphtol-As-BI-phosphate was used as a substrate and the coupling salt reaction was carried out with hexazotized pararosaniline. Counterstaining was performed by haematoxylin.

2.2.4.4.8. Scanning Electron Microscopy

Polymer-cell samples were prepared as described in a previous section. At the end of 21 and 29 days culture period, samples were fixed at 4 °C in 2.5% glutaraldehyde, 2% paraformaldehyde and 0.1 M sodium cacodylate buffer (pH 7.4) overnight. They were washed and refrigerated in 0.1 M of sodium cacodylate buffer (pH 7.4) until processed for SEM. Before use, they were rinsed with deionized water

and stored in a deep freezer (-80 °C). Before SEM observation, samples were freeze-dried for 8h and coated with gold. SEM was carried out in a Leitz (Germany), Model AMR 1000 SEM.

2.2.4.4.9. Confocal Microscopy

The mineralized parts of the bone matrix produced by the osteoblasts were observed under the confocal microscope. For that purpose, tetracycline (3 μg/mL), used as a fluorescent dye, was added in the osteoblast culture 24 h before determination of mineralization. Following a rinse in PBS and replacement with fresh media, the cell cultures were examined using confocal microscope (Zeiss LSM Pascal (Germany), Carl Zeiss). Depth projection micrographs were constructed from 4 horizontal image sections through the cultures.

CHAPTER 3

RESULTS AND DISCUSSION

3.1. Characterization of Support Material

3.1.1. Morphology of Foams with Scanning Electron Microscopy (SEM)

The surface characteristics, average pore sizes and the pore distribution of the untreated and unloaded, sucrose loaded, and oxygen plasma treated PHBV8 (4, 6, and 8 %, w/w) foams, Gelfix® and Gelfix®-calcium phosphate foams were observed by SEM.

The pore size and the pore distribution are quite important parameters for cell growth inside the matrices. Since osteoblasts can not grow without cell to cell contact, the average sizes of the pores should be at least 3 times bigger (>100 μm) than that of the cells so that a single cell can find a chance to establish contact with the others. It was found out from the SEM that as the polymer concentration

increased from 4% to 8%, untreated and unloaded PHBV8 had a more ordered, compact and smooth surface (Figures 3.1 a - c). The amount of the pores were not sufficient enough for osteoblast growth.

In order to obtain more porous foams, salt (NaCl) (50-100 μm) or sucrose crystals (75-300 μm or 300-500 μm) were loaded into the structure during foam preparation and then they were leached out leaving their locations empty. Salt crystals made the surface more porous than the unloaded ones (Figure 3.2). However, the size of the pores were not large enough for a cell growth inside the polymer.

After sucrose leaching, the number of the pores inside the foams increased (Figures 3.3 a and b). Two different sizes of the crystals were loaded inside the polymer (75-300 μm or 300-500 μm), respectively. Both large and small size sucrose loaded foams allowed cell growth but it was observed (Section 3.2.2.2) that matrices with the larger pore size (300-500 μm) provided a better osteoblast growth environment.

In the case of oxygen rf-plasma treated PHBV8 foams, a more porous and hydrophilic structure than that of the untreated ones was obtained. Before treatment, the surfaces of the foams were covered with a thin polymer film due to solvent evaporation method. The surface texture of the foams changed upon treatment as seen in the Figures 3.4 a - d. This could be explained by the etching of the very top layer of the membranes thus exposing the pores created by sucrose leaching.

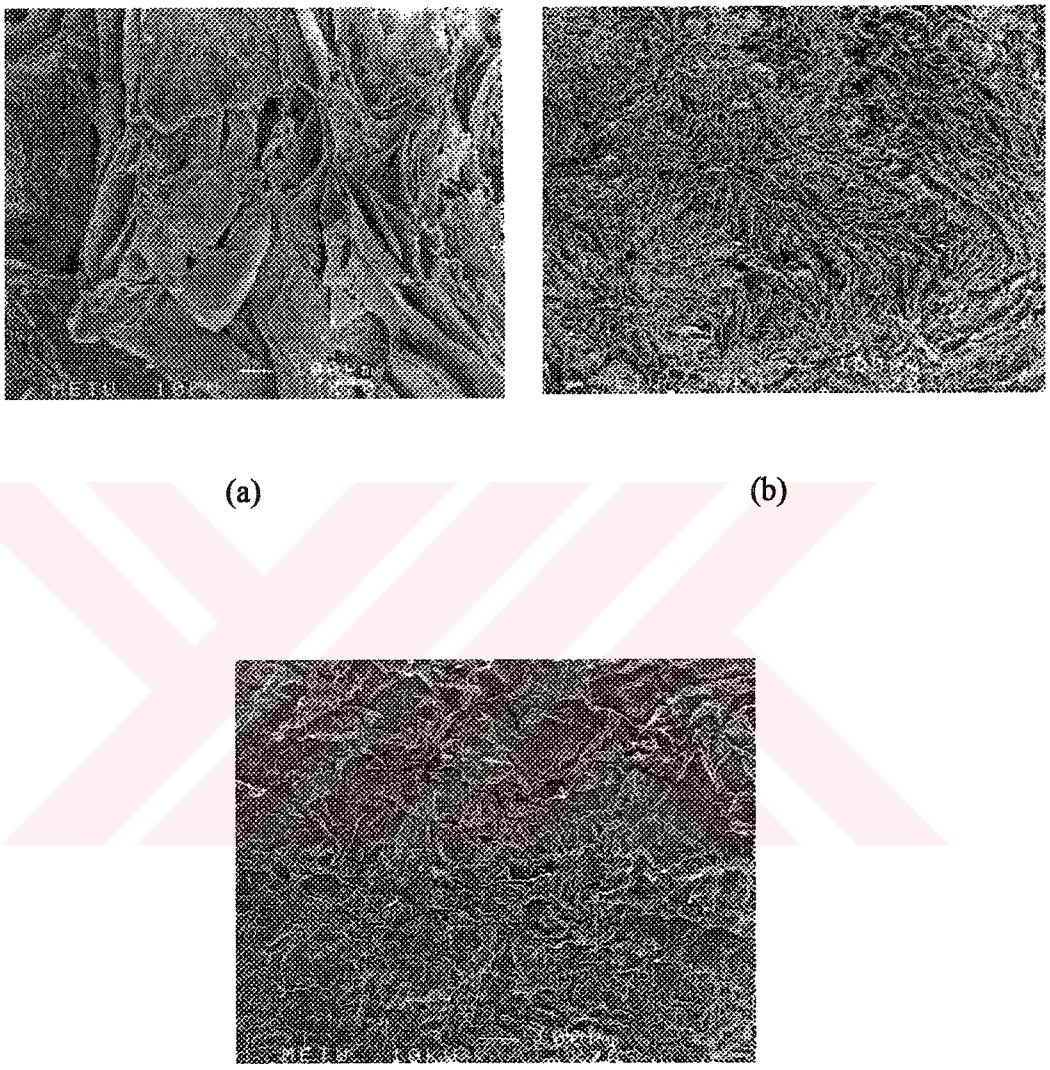

Figure 3.1. Scanning electron micrographs of untreated PHBV8 foams (no sucrose leaching to create pores), with different concentrations of the chloroform: dichloromethane solution of the polymer used in foam preparation: a) 4 %, b) 6 %, c) 8 %.

Figure 3.2. Scanning electron micrographs of untreated PHBV8 (6 %, w/w) foam with NaCl-leaching.

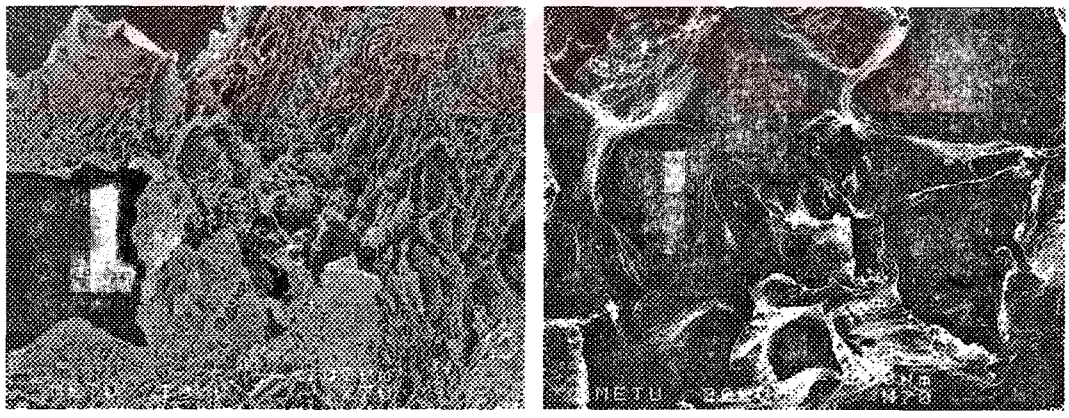

(a) (b)

Figure 3.3. Scanning electron micrographs of untreated PHBV8 (6 %, w/w) foams with sucrose-leaching. Sucrose size range : a) (75-300 μm), b) (300-500 μm).

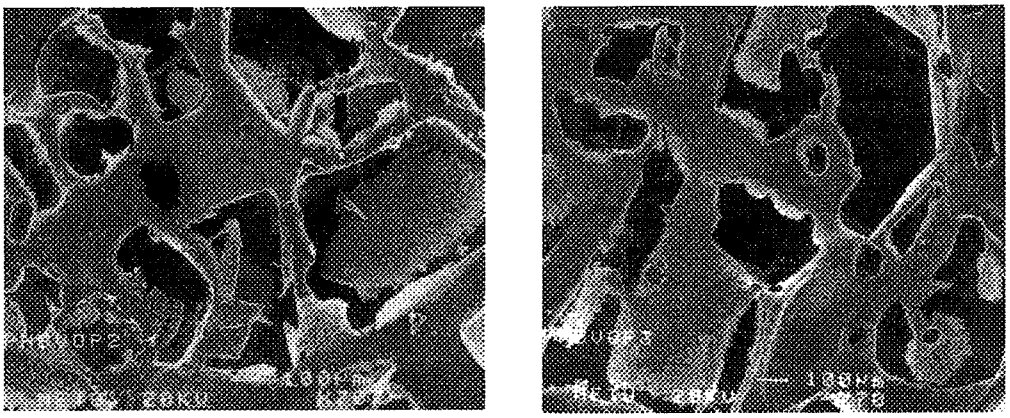

(a) (b)

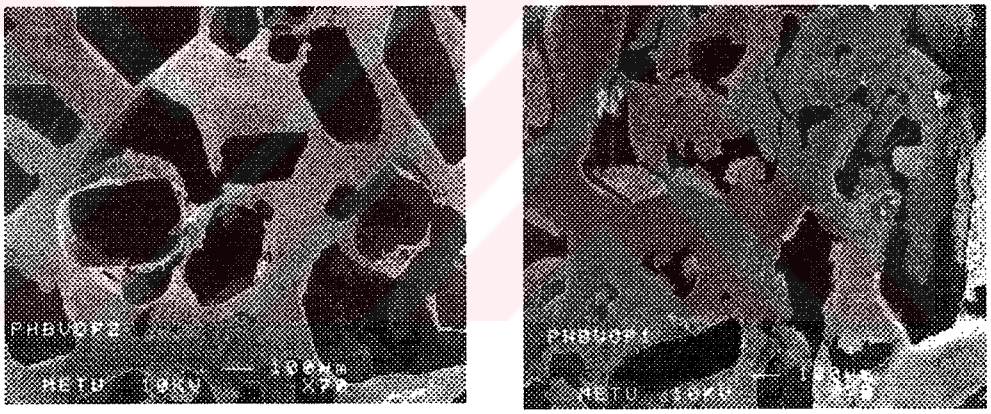

(c) (d)

Figure 3.4. Scanning electron micrographs of rf-oxygen plasma treated PHBV8 (6 %, w/w) foams with sucrose-leaching (300-500 μm). Treatment conditions: (a) 50 W 10 min, (b) 50 W 20 min, c) 100 W 10 min, d) 100 W 20 min.

Scanning electron micrography of untreated and calcium phosphate containing Gelfix® were also carried out (Figures 3.5 a and b). They both had porous structures but the untreated one appears to have a more delicate structure with a finer matrix.

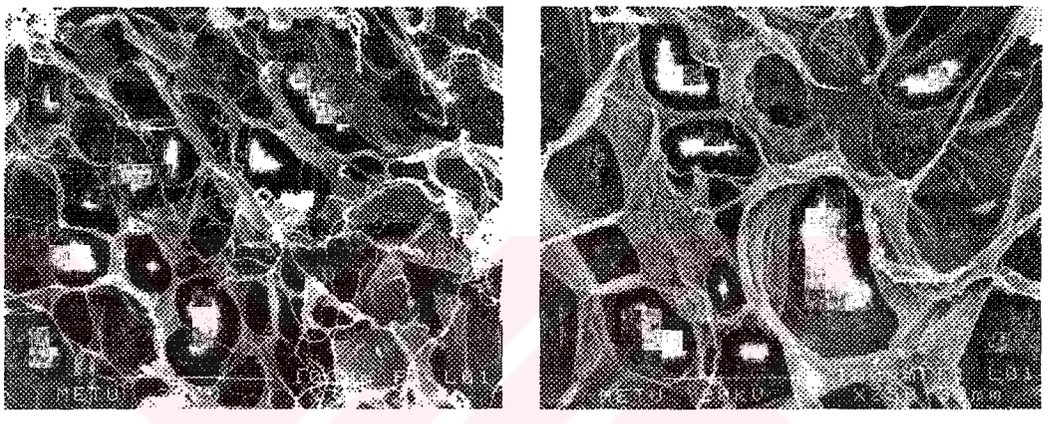

(a) (b)

Figure 3.5. Scanning electron micrographs of lyophilized collagen (Gelfix®) foams : a) Untreated Gelfix®, b) Calcium Phosphate loaded Gelfix®.

3.1.2. SEM Coupled with Energy Dispersive Spectra (SEM-EDS)

The presence and the ratio of calcium phosphate in Gelfix®-calcium phosphate matrix was determined by the EDS attachment of the SEM. Figure 3.6 a shows untreated Gelfix® (with practically no peaks except the gold of the conductive coating applied during SEM sample preparation) and the presence of the peaks due to

calcium and phosphorus atoms can be observed in Figure 3.6 b. In the calcium phosphate loaded Gelfix sample, the ratio of calcium over phosphorus was found to be 2.26 in the Gelfix®-calcium phosphate matrix. This is much higher than the targeted 1.67, a ratio specific for hydroxyapatite but similar to the results of a calcium phosphate deposition on gelatin membrane (2.33) (Yaylaoğlu et al., 1999). Thus, Gelfix-CaP construct might not closely mimic the natural bone but it probably will be much more durable than alternative constructs.

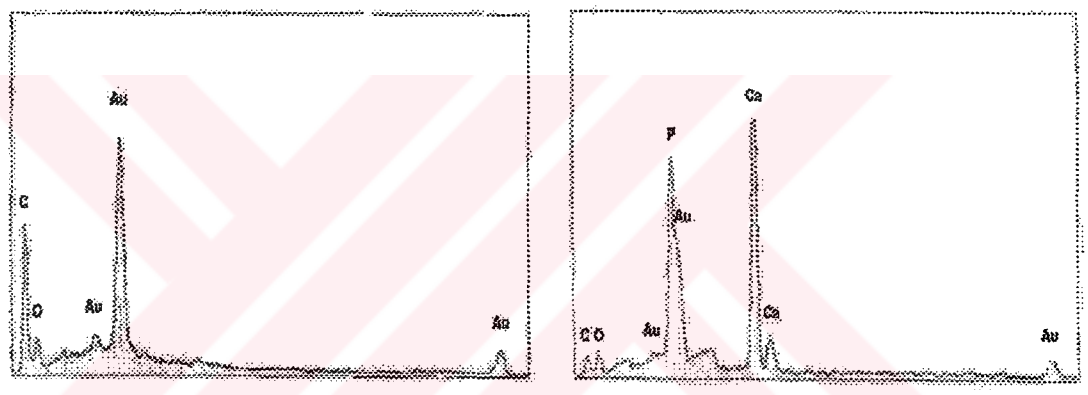

Figure 3.6. SEM coupled with Energy Dispersive Spectra (SEM-EDS) of lyophilized collagen (Gelfix®) foams : a) Untreated Gelfix®, b) Calcium Phosphate loaded Gelfix®.

3.1.3. Porosity Analysis

Image analysis was carried out to characterize the constructs in terms of their porosity. More specifically the aim was to calculate the average pore size and

the pore distribution of the matrices. They were examined using the Scion Image Analysis Program by NIH.

Image analysis results showed that the porosity (fraction of the surface that is void) of the untreated and unloaded PHBV8 (4, 6 and 8%) were 0.563, 0.428, and 0.368, respectively. Their pore size distributions were homogeneous (Figures 3.7 a - c). The porosities of (a) untreated and large sucrose loaded (300-500 μm) PHBV8 (6 %,w/w), (b) untreated and small sucrose loaded (75-300 μm) PHBV8 6%, (c) untreated and sodium chloride loaded (>150 μm) PHBV8 6%, and (d) oxygen plasma treated PHBV8 6% (100 W 20 min) were found as 0.694, 0.396, 0.420, and 0.656, respectively. Image analysis results showed that porosities of untreated and large sucrose loaded (300-500 μm) PHBV8 (6 %, w/w) and oxygen plasma treated PHBV8 6% (100 W 20 min) were more or less the same and their porosities were higher than that of others. Therefore, they were expected to allow better osteoblast growth inside their matrices.

The porosities of untreated gelfix, and Gelfix-CaP were found as 0.610 and 0.575, respectively. Although the porosity of Gelfix-CaP is somewhat less than that of untreated one, it allows better osteoblast growth (see Section 3.2.2.4).

The pore size distributions could also be obtained from the same analyses. The influence of polymer concentration in foam preparation solution can be studied using Figures 3.7 a – c, and 3.8 a – d. Although not conclusive by itself the data reveals that with the high polymer concentration foams, the pores are at the low end of the scale while with lower concentration foams, the number of pores (including at the lower end) and their sizes are higher.

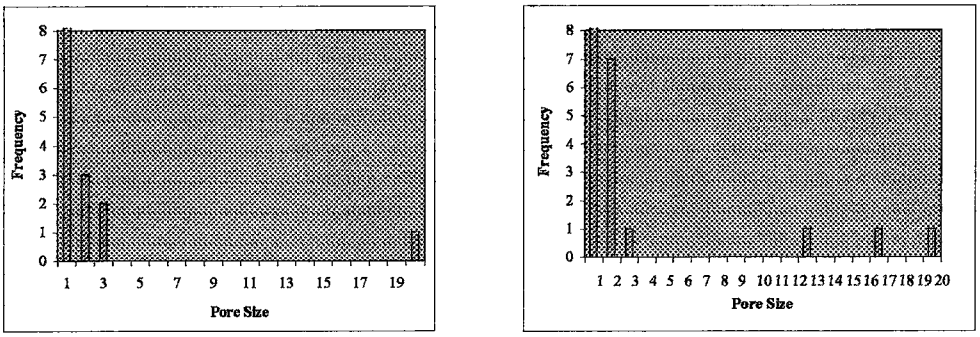

(a) (b)

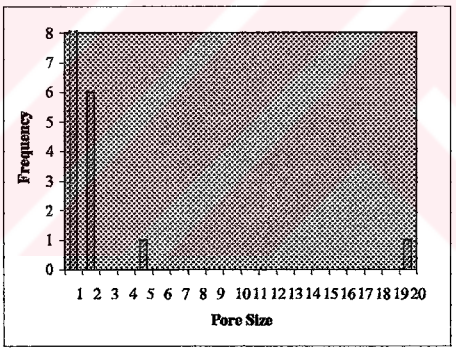

(c)

Figure 3.7. Pore size distribution of untreated PHBV8 foams (no sucrose loaded to create pores) : a) 4 %, b) 6 %, c) 8 %.

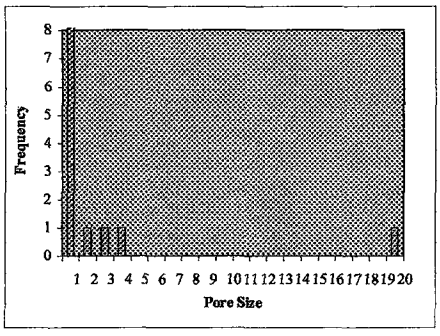

(a)

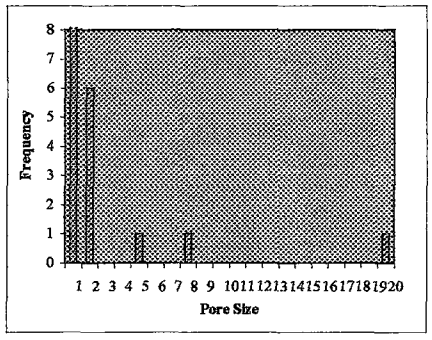

(b)

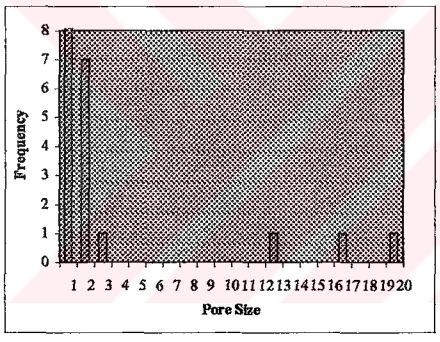

(c)

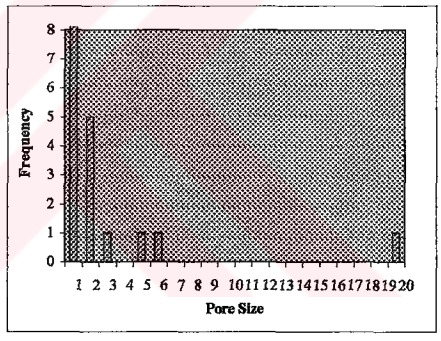

(d)

Figure 3.8. Pore size distribution of PHBV8 (6 %, w/w) foams with: a) untreated sucrose loaded (300-500 μm), b) untreated sucrose loaded (75-300 μm), c) untreated NaCl-leaching (< 150 μm), d) rf-oxygen plasma treated PHBV8 (6%, w/w) (100 W 10 min).

The most effective use of pore size analysis with Scion Image is achieved with Gelfix foams. As can be seen in Figures 3.9 a and b, the number of

pores are significantly higher than any other material tested in this study. It can also be observed that calcium phosphate production in the matrices distinctly decreases the number of pores on the material surface and even then, the sizes and the number are still higher than those obtained with PHBV.

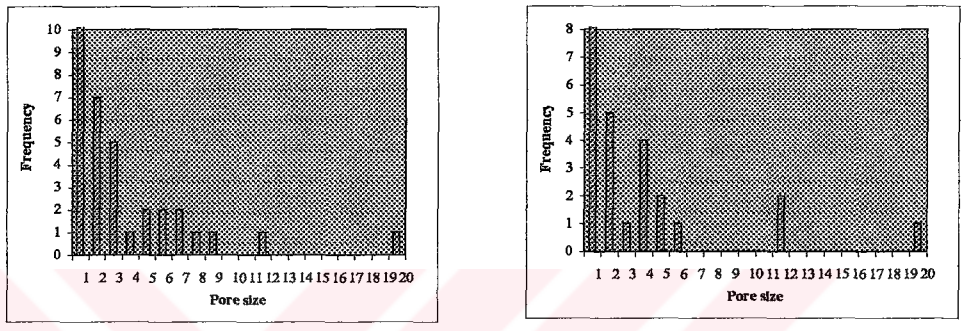

(a) (b)

Figure 3.9. Pore size distribution of lyophilized collagen (Gelfix®) foams : a) Untreated Gelfix®, b) Calcium phosphate loaded Gelfix®.

3.1.4. Void Volume and Density Calculations

Volume of pores inside the untreated large sucrose loaded PHBV8 (4, 6, and 8 %), oxygen plasma treated, large sucrose loaded (100 W 20 min) PHBV8 6%, untreated small sucrose loaded (75-300 μm) PHBV8 6%, untreated sodium chloride (NaCl) loaded PHBV8 6%, Gelfix®, and Gelfix®-calcium phosphate foams was determined (Table 3.1).

As the concentration of the PHBV8 increased from 4 to 8 %, volume of the pores inside the matrices decreased. Volumes of the untreated large sucrose loaded (300-500 μm) PHBV8 and oxygen plasma treated (100 W 20 min) large sucrose loaded PHBV8 were almost the same and higher than that of untreated small sucrose loaded (75-300 μm) PHBV8 6%, and untreated sodium chloride loaded PHBV8 6%. This is expected to give matrices a better chance for cell growth. The volume of the pores in Gelfix® is a little bit more than that of Gelfix®-calcium phosphate foams due to loading of calcium phoshate into the structure of the latter.

Table 3.1. Void volumes of various PHBV8 and Gelfix foams.

Foam Type	**Void Volume of Foam (mL/g foam)**
PHBV8 4%, LS	0.3663 ± 0.01239
PHBV8 6%, LS	0.2897 ± 0.01416
PHBV8 8%, LS	0.2207 ± 0.01991
PHBV8 6%, LS, OP	0.2856 ± 0.01223
PHBV8 6%, SS	0.1307 ± 0.02231
PHBV8 6%, Salt	0.1964 ± 0.01748
Gelfix-untreated	0.2658 ± 0.01549
Gelfix-CaP loaded	0.2548 ± 0.01552

LS: Large sucrose crystal loaded foam (300-500 μm), SS: Small sucrose crystal loaded foam (75-300 μm), OP: Oxygen plasma treated foam (100W 20min).

Foam densities of the same samples were also determined by pycnometry. The densities of the foams were calculated from these data (Table 3.2).

Table 3.2. Density of PHBV8 and Gelfix Foams.

Foam Type	**Density of Foam (g/mL)**
PHBV8 4%, LS	0.0515 ± 0.0096
PHBV8 6%, LS	0.0876 ± 0.0109
PHBV8 8%, LS	0.1064 ± 0.0083
PHBV8 6%, LS, OP	0.1160 ± 0.0101
PHBV8 6%, SS	0.2057 ± 0.0372
PHBV8 6%, Salt	0.0602 ± 0.0064
Gelfix-untreated	0.0726 ± 0.0087
Gelfix-CaP loaded	0.0798 ± 0.0094

LS: Large sucrose crystal loaded foam (300-500 μm), SS: Small sucrose crystal loaded foam (75-300 μm), OP: Oxygen plasma treated foam (100W 20min).

It was observed that as the concentration of the PHBV8 increased from 4 to 8 %, density of the matrices increased twice (from 0.0515 to 0.1064 g/mL) as was expected. Since there were more pores in the structure of the untreated large

sucrose-loaded (300-500 μm) PHBV8 and oxygen plasma treated (100 W 20 min) large sucrose loaded PHBV8, they were less denser than untreated small sucrose loaded (75-300 μm) PHBV8 6% foams. The density of Gelfix®-calcium phosphate foam (0.0789 g/mL) was slightly more than Gelfix® (0.0726 g/mL) because of the presence of the calcium phosphate in the structure and also possibly due to the processing procedure.

3.1.5. Water Contact Angle Measurements

The wettabilities of the untreated and rf-oxygen plasma treated PHBV8 and Gelfix® matrices were assessed by sessile drop method using Cam-Micro (Tantec Inc., USA). A droplet of water was placed onto the foams and contact angle study was carried to observe the degree of hydrophilicty. However, due to the high porosity and high hydrophilicity of the foams both in the bulk and on the surfaces, the applied water droplet spread on the surface and it was not possible to determine the contact angles.

3.1.6. Degradation of PHBV8 and its Quantification via pH Changes and Gravimetry

For the degradation study, unloaded PHBV8 (4, 6, and 8 %, w/w), and sucrose loaded PHBV8 foams were used. All measurements were expressed as means ± standard deviation (sd) relative to the initial values. Matrices prepared from PHBV 4 % led, in 180 days, to a pH decrease of 0.19 pH units when they were in

unloaded (dense) foam form and 0.18 pH units for sucrose loaded PHBV foams. Meanwhile the 6 % and 8 % led to pH decreases of 0.16 and 0.20 units for unloaded, and 0.17 and 0.20 units for sucrose loaded PHBV8 in 180 days, respectively. This pH decrease is an indication of the degradation extent and therefore, the sample that leads to the largest pH drop would have been the one that has degraded the most (Figures 3.10 a - e). The data presented, however, did not indicate any significant difference between the samples tested.

Density changes for the unloaded and sucrose loaded 4, 6, and 8 % samples were almost the same during the 180 day period. What is more significant is that there was no perceptible change in the first 120 days and then a 2 fold decrease was observed during the following 60 days (Figures 3.11 a and b).

Sample thicknesses initially increased with time possibly due to degradation of the sample cores and drawing of the aqueous medium into the structure. This, however, changed at around 120 days and the sample thickness gradually decreased until 180^{th} day.

Sample weights also changed in a similar manner. After 120 days in the medium weight loss started to be noticable (Figure 3.11 c and d). In summary it appears that the samples absorb the solvent (water) and strain by swelling until 120 days and then chain scission starts shortening the chains and causing the changes density, weight and thickness.

These indicate that the microenvironment of the loaded cells will become less restrictive in time (at least after the initial 3 months) and, therefore, increases in cell numbers will not be excessively hindered by space limitation.

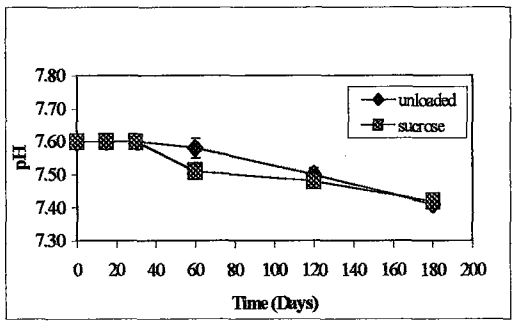

(a)

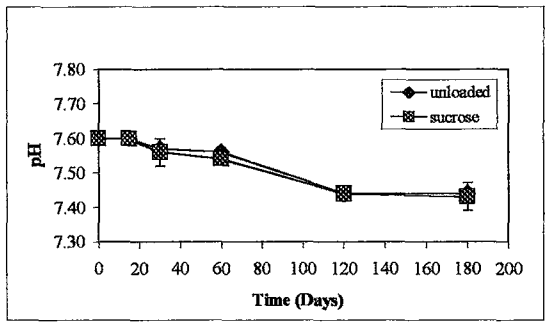

(b)

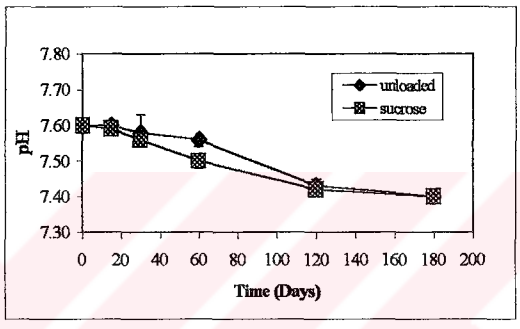

(c)

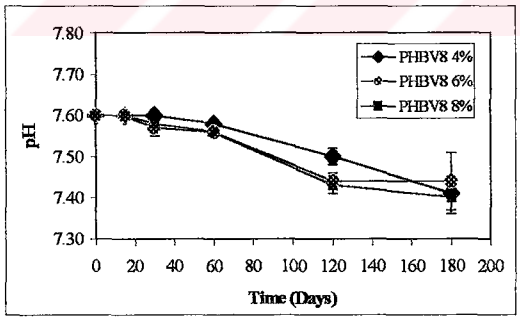

(d)

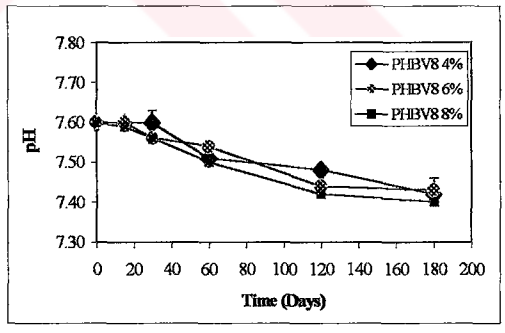

(e)

Figure 3.10. Change in the pH of the medium as an indication of degradation of PHBV8 foams : a) 4 %, b) 6 %, c) 8 %, d) unloaded PHBV8, e) sucrose loaded PHBV8.

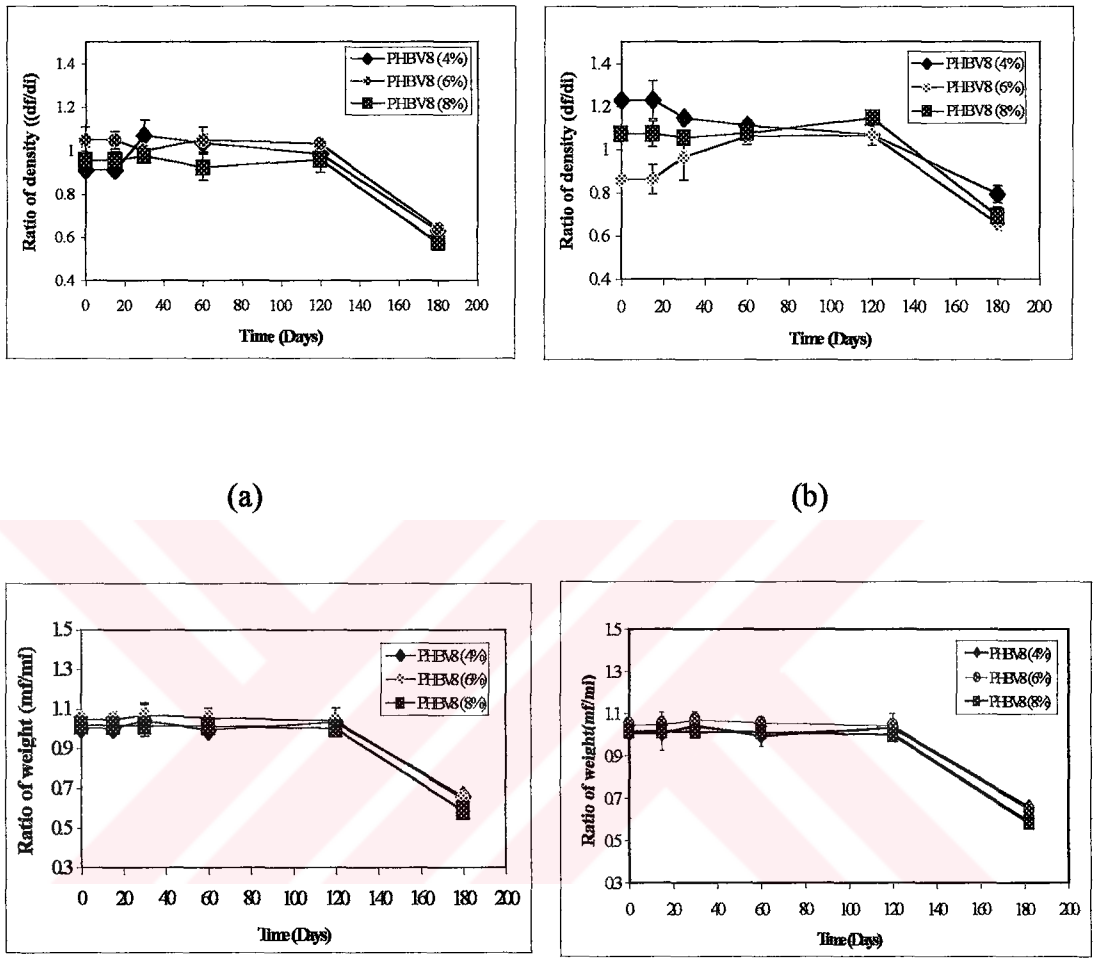

Figure 3.11. Degradation of PHBV8 foams. Ratio of (final to initial) density (df/di) vs time graph for: a) unloaded PHBV8, b) sucrose loaded PHBV8. Ratio of (final to initial) weight (mf/mi) vs time graph for: c) unloaded PHBV8, and d) sucrose loaded PHBV8.

3.2. *In Vitro* Osteoblast-Biomaterial Interaction Studies

3.2.1. Osteoblast Characterization

3.2.1.1. Microscopic Evaluation (Light Microscopy)

Osteoblasts were isolated from Wistar rats and cultured on TCPs (Figures 3.12 a and b). After the first passage, cells were visualized by inverted phase contrast microscope (Olympus MO81, Japan).

Osteoblasts are differentiated cells, usually derived from osteoprogenitor cells. They are mobile. They change shape and size and appear with the vascular tissue. The main function of the osteoblasts is the synthesis and secretion of the organic matrix of bone. They also control electrolyte fluxes between the extracellular fluid and the osseous fluid and may influence the mineralization of bone matrix through the synthesis of organic matrix components of bone and the production of matrix vesicles. Moreover, some systemic hormones such as parathyroid hormone and local cytokines may stimulate osteoblasts to release mediators that activate osteoclasts (Buckwalter et al. 1995). Inverted microscope was used to observe the expression of the osteoblast phenotype after 2 and 6 (confluency) days of incubation (Figure 3.13 a and b). On the surface, cells exhibited spindle-like morphology and had a cell diameter of 10-30 μm. They contact each other, grow and after 10 days of isolation they reach confluency in which no empty space could be seen on the surface of the TCPs.

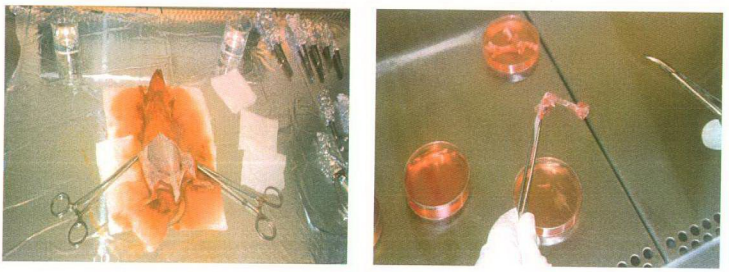

(a) (b)

Figure 3.12. Isolation of osteoblast cells from Wistar rat bone marrow : a) Before removal of femur and tibia, b) Before isolation of bone marrow .

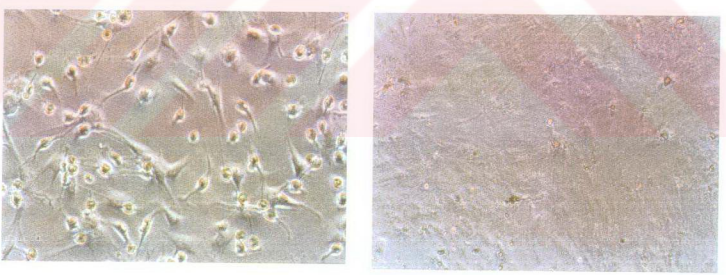

(a) (b)

Figure 3.13. Stages of *in vitro* growth of primary osteoblast cells : a) 2 days of incubation (x 20), b) 6 days of incubation (full confluency) (x 20).

3.2.1.2. Determination of Alkaline Phosphatase Activity by Spectroscopic Method

The enzyme activity in the osteoblast cells was demonstrated by the alkaline phosphatase assay using a spectrophotometric technique. 2-D osteoblast cultures of second, third and fourth passages in T-75 flasks were studied for the production of alkaline phosphatase (ALP) activity of the cells.

Table 3.3 shows the presence of bone specific ALP into the samples. The amount of ALP in the medium (2 U/L) was not significant. Since it contains serum, this ALP possibly comes from the serum.

Table 3.3. Spectroscopic ALP Assay of osteoblasts in different passages after 7 days of incubation (n = 3).

Passage number of cells	ALP activity (U/L)
Medium	2 ± 0
Serum	2 ± 0
2	395 ± 4
3	200 ± 1
4	130 ± 6

The presence of bone specific ALP indicates osteoblastic cell growth. All cell passages expressed high alkaline phosphatase activities and it was observed that increase in serial passage number resulted in a decrease in ALP activity (from 395 to 130 U/L). In the case of primary cell cultures, cells tend to lose their special

characteristics as the number of passages increases. Loss of phenotype may be observed when diploid cells cultured for a long time and this may be the reason why the ALP activity of the 2nd passage was found to be higher than that of 3rd and 4th passages (Figure 3.14).

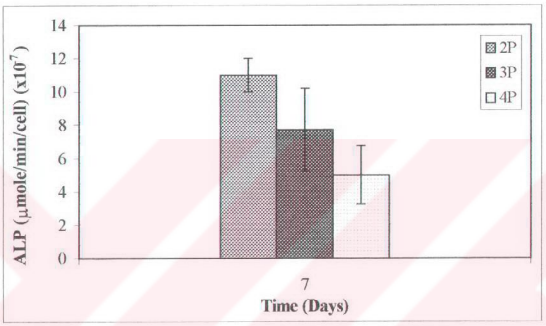

Figure 3.14. Alkaline phosphatase activity of osteoblasts in different passages (2P, 3P, and 4P) after 7 days of incubation.

3.2.1.3. Determination of Alkaline Phosphatase by Electrophoresis

Same samples studied in the ALP spectrophotometric assay (Section 2.2.4.3.2) were used to visually show the presence of ALP via electrophoresis. Two fibroblast cell and human serum samples were also used as a control and ALP electrophoresis was carried out.

As was expected, bone ALP was not detected in the undifferentiated cells (wells 5 and 6) (Figure 3.15). On the other hand, the presence of bone specific ALP can be easily observed in the differentiated samples (wells 2, 3, 4, and 7). The intensity of the bands is a sign of successful osteoblastic cell growth. The decrease in intensity from well 2 to 4 is a further proof (in addition to ALP activity test) of loss of special characteristics upon increase in passage number of the osteoblasts.

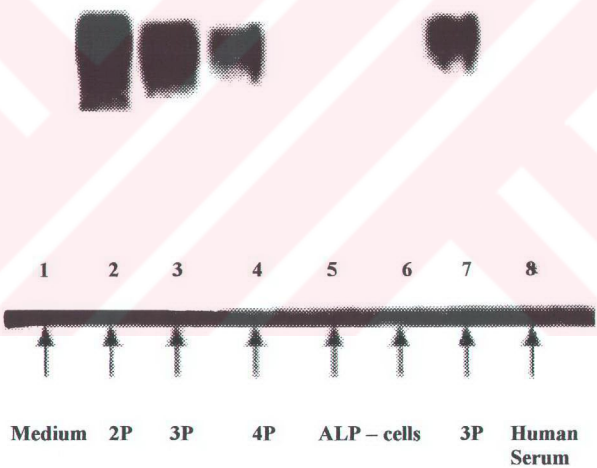

Figure 3.15. Alkaline phosphatase electrophoresis of osteoblast cultures.

Wells: **1.** Medium; **2-4.** cells at passages 2, 3, and 4; **5** and **6.** undifferentiated cells; **7.** a repeat of passage 3 sample; **8.** human serum.

3.2.1.4. Determination of Osteocalcin

Samples used in the previous two tests were used in the determination of osteocalcin. The phenotype of primary isolated rat osteoblasts was confirmed by measuring the presence of bone-related proteins such as osteocalcin.

The presence of osteocalcin indicates osteoblastic cell growth. All cell passages expressed osteocalcin activities and it was observed that increase in serial passage number resulted in a decrease in osteocalcin activity (from 80 to 39 ng/cell, $x10^{-6}$) as it was observed in ALPase experiment (Figure 3.16). Therefore, 2nd passage gave the best results in terms of both ALPase and osteocalcin activities.

Phenotype evaluation during serial subculture is essential for the selection of the appropriate cell population to be used in *in vitro* studies. Because of that osteoblasts in 2nd passage were used in the rest of the study.

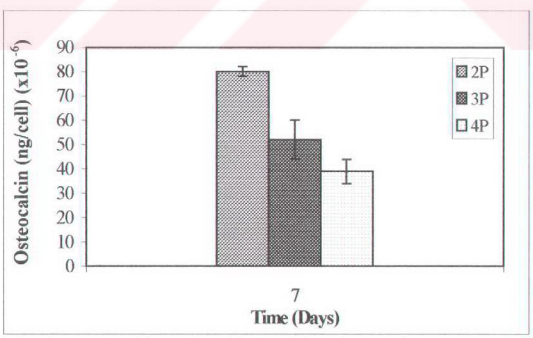

Figure 3.16. Osteocalcin secretion of osteoblasts in passages 2P, 3P, and 4P.

3.2.1.5. Cell Growth Kinetics

The log and plateau phases observable on the cell growth kinetic plots give important information about the cell line, such as the population doubling time and saturation density (the maximum cell density achieved in plateau). Measurement of the population doubling time is used to quantify the response of the cells towards different inhibitory or stimulatory culture conditions, such as variations in nutrient concentration, hormonal effect, or toxic drugs. It is also a good indicator of the culture during serial passage and enables the calculation of cell yields and the dilution factor required at subculture. In this study, population doubling time was found to be 50 ± 2 h for the osteoblast cells (Figure 3.17). Cells reached growth saturation after about 120 h of incubation.

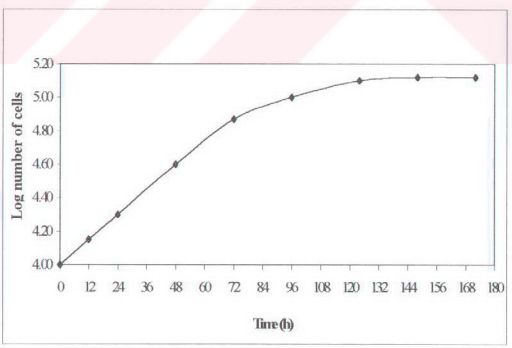

Figure 3.17. Growth kinetics of osteoblast culture ($1x10^4$ cells/mL).

3.2.1.6. Western Blot for Integrin

Integrins are cell-surface proteins that mediate cell adhesion, proliferation, migration, differentiation, and apoptosis (Yamada and Miyamoto, 1995). Several integrin subunits including α_1, α_2, α_3, α_4, α_5, α_v, β_1, and β_5 have been detected in bone cells (Saito et al. 1994). $\alpha_1\beta_1$, $\alpha_2\beta_1$, $\alpha_3\beta_1$, and $\alpha_v\beta_1$ bind type I collagen in osteoblasts (Ganta et al. 1994). Integrin receptor binding and clustering culminate in the formation of focal adhesion sites where integrins connect the cytoskeleton and the ECM.

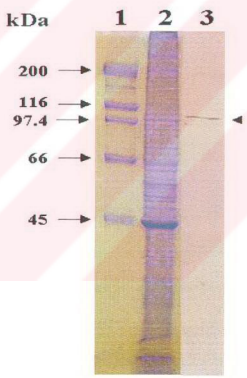

Figure 3.18. Western blot for Integrin.

Lane 1, Molecular weight marker (Broad range, BioRad, Ca, USA); **Lane 2**, SDS PAGE of cellular proteins of osteoblasts; **Lane 3**, Integrin band formed after incubation with anti-b-1-Integrin Mab (Clone DF5, ICN, USA).

2-D osteoblast culture of third passage was examined for integrin β_1 expression by western blot. After incubation with anti β_1 integrin Ab, formation of β_1 integrin (100 kDa) band was observed in Figure 3.18. This band indicates the presence of β_1 integrin which is also one of the indicators of osteoblast phenotype.

3.2.1.7. Determination of Cell Viability by Cell Titer 96^{TM} Nonradioactivity Cell Proliferation Assay (MTS Assay)

Different concentrations of the osteoblast cells ($1x10^4$, $2.5x10^4$, $5x10^4$, $10x10^4$, $15x10^4$, $20x10^4$, $30x10^4$, $40x10^4$, $50x10^4$) were seeded on a 96 well Elisa plate to determine the cell viability and construct a calibration curve (Table 3.4 and Figure 3.19). This calibration curve was used in the determination of the cell concentration inside the matrices and by this way, it was possible to quantitate the cells seeded inside the matrices.

Table 3.4. MTS assay for different concentrations of osteoblasts

Number of cells	Mean OD (490nm)
Blank	0.491
10,000	0.016
25,000	0.060
50,000	0.116
100,000	0.280
150,000	0.357
200,000	0.507
300,000	0.699
400,000	0.925
500,000	1.169

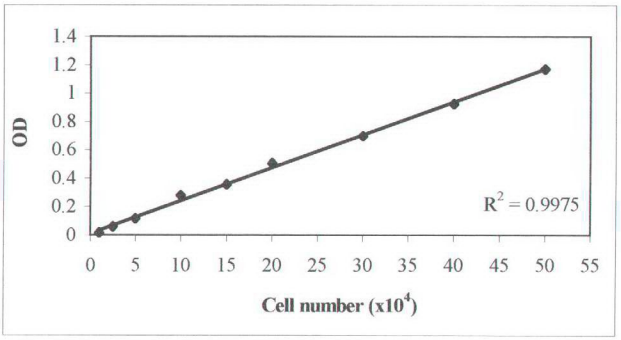

Figure 3.19. MTS calibration curve for osteoblast determination (An OD490 vs log Cell Number $x10^5$ plot).

3.2.2. Seeding of Polymeric Foams and Films with Osteoblasts

3.2.2.1. Osteoblast Growth on Polymeric Films

PHBV8 films prepared by solvent evaporation of chloroform solutions and not subjected to any further treatment, were seeded with cells of concentrations of $1x10^4$ and $10x10^4$ cells/mL and incubated for 7 days at 37 °C in a CO_2 incubator. At the end of seven days, MTS assay was applied and cell growth on the PHBV8 films was observed (Table 3.5 and Figure 3.20). The data showed the presence of osteoblast growth on PHBV8 films. PHBV8 had no toxic effect on growth of osteoblasts. The exact amount of the cells after 7 days of incubation on the PHBV8 films was determined from the calibration curve (Section 3.2.1.6.) derived from the MTS assay of different concentrations of cells.

Table 3.5. Determination of viability of osteoblasts on PHBV8 films after 7 days of incubation by MTS assay

	Mean OD (490 nm)	**Cell Number**
Medium+PHBV8	0	-----
Medium	0	-----
10,000 cells/mL	0.050	20,000 ± 4000
100,000 cells/mL	0.348	150,000 ± 10000

Figure 3.20. Inverted light microscopy of osteoblast growth on PHBV8 film with a seeding density of 10,000 cells/mL after 7 days of incubation (x 20).

3.2.2.2. Osteoblast Growth on Polymeric Foams with Different Pore Sizes

6 and 8 % PHBV8 foams were prepared as described (in Section 2.2.1.3). Two different sized crystals (small size-75-300 μm; large size- 300-500 μm) were used to study the effect of pore size on osteoblast growth. Foams seeded with osteoblast at concentrations of $1x10^5$, $5x10^5$ and $10x10^5$ cells/mL were incubated for 7 days in a CO_2 incubator at 37 °C. MTS assay was used to determine the cell density inside the polymeric matrices (Tables 3.6).

The results showed that cell numbers increased more on large pore size foams (made by 300-500 μm sucrose crystals) than on small pore size foams (75-300 μm sucrose crystals).

Moreover, lower concentration, PHBV8 (6 %, w/w), foam seemed to be a better support matrix than the higher concentration, PHBV8 (8 %, w/w), foam.

During seeding, cell concentration of 500,000 cells/mL seemed to be the ideal loading condition because the higher concentration (1,000,000 cells/mL) seeding showed less growth than with seeding with 500,000 cells/mL. This, however, is not only due to cell crowding during seeding. The difficulty of loading such a high amount of cell onto the polymer is caused by the need to use a larger volume of cell suspension which lead to the run-off of this fluid. Thus the actual loading is significantly lower than planned. The leaked cells proliferated on the polystyrene (TCPs) plate beneath the polymer thus not contributing to the counts.

One also has to consider that the free cells also showed a similar optimum at 500,000 cells/mL, however, the level of change is negligible indicating that the restrictions on the cells within the foams are significantly greater.

Table 3.6. MTS assay for osteoblast growth on PHBV8 with different pore sizes (n = 3).

PHBV preparation concentration and sucrose type	Cell number (x 10^3) after 7 days of incubation		
	Initial $1x10^5$	Initial $5x10^5$	Initial $10x10^5$
Free cells	900 ± 40	1202 ± 70	984 ± 50
6% SSC	160 ± 6	646 ± 10	625 ± 10
6% LSC	189 ± 8	680 ± 5	629 ± 10
8% SSC	107 ± 7	607 ± 8	612 ± 9
8% LSC	156 ± 4	642 ± 4	620 ± 10

SSC : small sucrose crystal (75-300 μm)-PHBV8; LSC : large sucrose crystal (300-500 μm)-PHBV8; with no surface treatment.

3.2.2.3. Osteoblast Growth on Polymeric Foams with Different Surface Treatments

The surfaces of the large sucrose loaded PHBV8 matrices were treated with rf-oxygen plasma (100 W 10 min) and osteoblast growth was studied on different PHBV8 matrices (6 and 8 %, w/w) (Table 3.7).

The influence of foam preparation concentration was similar to that observed in Table 3.6. Higher the polymer concentration lower was the cell concentration.

Optimum seeding concentration also peaked at 500,000 cells/mL decreasing on both sides.

Finally, the rf-plasma treatment positively influenced cell seeding efficiency causing increases ranging between 6 to 24 % (observed with the lowest seedings). Since oxygen plasma treatment makes the surface more hydrophilic, it probably provides a better osteoblast growth microenvironment than untreated PHBV8.

In order to study the effect of extent of oxygen plasma modification of the foams on osteoblast cell growth inside the PHBV8 matrices, foams were treated at different levels (50W for 10min, 50W for 20min, 100W for 10min and 100W for 20min) as described in section 2.2.1.4. Osteoblast seeded foams ($2x10^5$ cells/mL) were incubated for 14 days in CO_2 incubator. Untreated PHBV8 was used as a control in this experiment. MTS assay was carried out to determine the number of cells within the matrices (Table 3.8).

Table 3.7. MTS assay results for osteoblast growth on PHBV8 (n = 3).

After 7 days of incubation; with rf-oxygen plasma treatment (100 W 10 min)

PHBV preparation concentration and sucrose type	Cell number ($x10^3$) after 7 days of incubation		
	Initial $1x10^5$	Initial $5x10^5$	Initial $10x10^5$
Free cells	900 ± 40	1202 ± 70	984 ± 50
6% Untreated	189 ± 6	680 ± 4	629 ± 9
8% Untreated	156 ± 6	642 ± 9	620 ± 8
6% Oxygen plasma treated	240 ± 8	727 ± 5	663 ± 10
8% Oxygen plasma treated	184 ± 8	684 ± 4	642 ± 7

Table 3.8. Osteoblast growth on PHBV8 foams with different oxygen plasma treatments as determined with MTS assay (After 7 days of incubation).

Sample Type	OD_{490}	Cell Number*
Free cells	0.810	350,000 ± 10500
Untreated PHBV	0.690	300,000 ± 9300
PHBV-50W 10min	0.693	300,000 ± 5000
PHBV-50W 20min	0.806	350,000 ± 8500
PHBV-100W 10min	0.919	400,000 ± 10000
PHBV-100W 20min	0.852	370,000 ± 8100

* Initial seeding 250,000 cells per sample

It is observed that untreated and the least treated foams allowed lowest populations of osteoblasts within their structures. As the treatment extent increased the level of occupation of the foam structure increased peaking at 100 W for 10 min. For the free cells, it was found that cell number was much lower than observed under similar conditions. This makes the results obtained more valuable since some OD values are even higher than those of the free cells indicating that the matrices provided a very suitable environment for cell growth.

3.2.2.4. Determination of Viability on Polymeric Foams

At the end of 21 and 29 days of incubation at 37 °C in a CO_2 incubator, osteoblast seeded, large sucrose loaded (300-500 μm) PHBV8 foams were subjected to MTS assay. Cell viability was also determined inside the Gelfix foams after 7 days of incubation in a CO_2 incubator. Further incubation could not be possible especially with the untreated Gelfix due to its rapid degradation in an aqueous environment.

After 21 days of incubation cell number increased from 150,000 cells/mL to 200,000 cells/mL for untreated PHBV8 and 220,000 cells/mL for oxygen plasma treated (100 W 10 min) PHBV8 (Table 3.9). At the end of 29 days of incubation cell numbers of the both foams were further increased (270,000 cells/mL for untreated and 350,000 cells/mL for oxygen plasma treated PHBV8 foams). These data show us that oxygen plasma treated PHBV8 is definitely a more suitable matrix material for osteoblast growth.

Due to the rapid degradation problem, Gelfix foams could only be incubated for 7 days in a CO_2 incubator. Although, the initial cell density was

150,000 cells, cell number did not increase as much (160,000 cells/mL) for untreated Gelfix. For the calcium phosphate loaded Gelfix the cell number was increased to 170,000 cells/mL after 7 days of incubation.

Table 3.9. Determination cell viability on PHBV8 and Gelfix foams by MTS assay.

Incubation Time (Days)	Polymer Matrix Preparation	Cell Number*
7	UT Gelfix	160,000 ± 4600
7	CaP-Gelfix	170,000 ± 12000
21	UT PHBV8	200,000 ± 15000
21	OP PHBV8	220,000 ± 9500
29	UT PHBV8	270,000 ± 6200
29	OP PHBV8	350,000 ± 9000

CaP-calcium phosphate; OP-oxygen plasma treated; UT-untreated. * Initial seeding 150,000 cells per sample.

3.2.2.5. Determination of Alkaline Phosphatase on Polymeric Foams

For the determination of the effect of the cell-substrate interaction on the production of alkaline phosphatase by cultured cells, cells were cultured for 21 and 29 days on a polymer scaffold. ALP activity expressed as μmol min^{-1} $cell^{-1}$ increased over time for all samples (Figure 3.21).

Both on days 21 and 29, the ALP activities of oxygen plasma treated (100 W 10 min) PHBV8 (3.6 and 4.8 μmol min^{-1} $cell^{-1}$, respectively) were higher than that of untreated PHBV8 (3.4 and 3.9 μmol min^{-1} $cell^{-1}$, respectively).

For the Gelfix foams, there was not a very significant difference between the untreated and calcium phosphate loaded ones (3.1 and 3.3 μmol min^{-1} $cell^{-1}$, respectively). This could be due to the short incubation (7 days) of the cells inside the Gelfix foams (Figure 3.22).

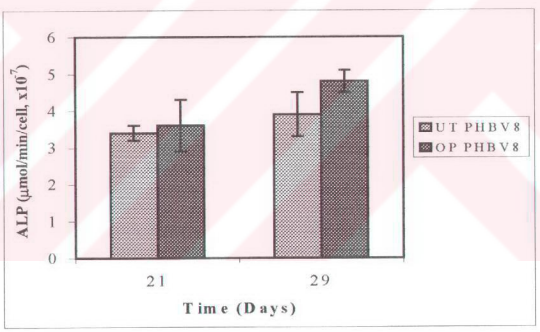

Figure 3.21. ALP activity of osteoblasts cultured inside the PHBV8 foams for 21 and 29 days (UT-untreated; OP-oxygen plasma treated).

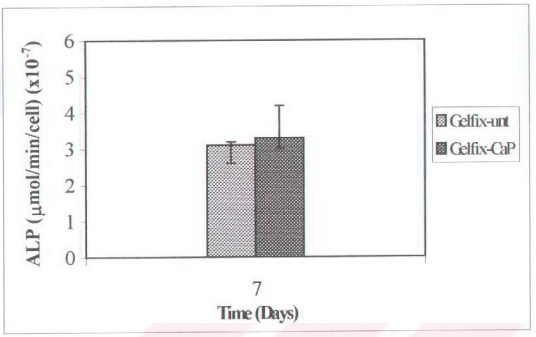

Figure 3.22. ALP activity of osteoblasts cultured inside the Gelfix foams for 7 days.

3.2.2.6. Determination of Osteocalcin on Polymeric Foams

Same samples in ALP activity experiment were used in the osteocalcin study. The osteocalcin secretion expressed as ng/cell $x10^{-6}$ increased from Day 21 to Day 29 for both the samples (Figure 3.23). The increase in the oxygen plasma treated (100 W 10 min) PHBV8 foams on Day 29 was very significant. Both on Day 21 and Day 29, osteocalcin secretion of the osteoblasts was higher in oxygen plasma treated (100 W 10 min) PHBV8 foams (25 and 66 ng/cell, $x10^{-6}$) than with untreated ones (22 and 30 ng/cell $x10^{-6}$). Figure 3.24 shows osteocalcin secretion of the cells on Gelfix foams. There was not a significant difference in osteocalcin secretion from untreated and calcium phosphate loaded Gelfix.

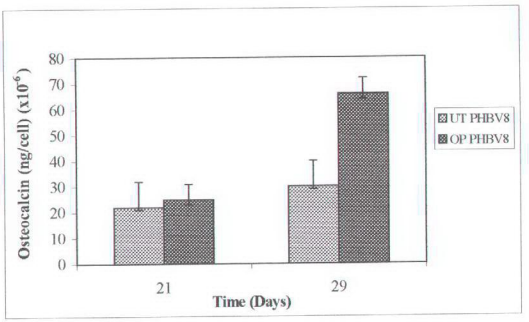

Figure 3.23. Osteocalcin activity of osteoblasts cultured inside the PHBV8 foams for 21 and 29 days (UT-untreated; OP-oxygen plasma treated).

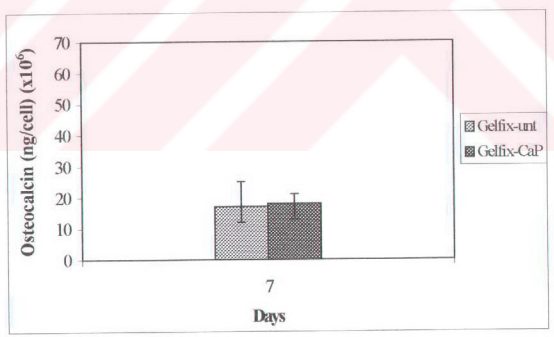

Figure 3.24. Osteocalcin activity of osteoblasts cultured inside the Gelfix foams for 7 days.

3.2.2.7. Determination of Mineralization (Histological Staining)

Osteoblast-foam (PHBV8 and Gelfix) constructs were prepared for histology after 7 days for Gelfix and, 21 and 29 days for PHBV8, in culture.

Figure 3.25 a and b (x10 and x20) shows osteoblasts in close contact with calcium phosphate crystals in calcium phosphate loaded Gelfix after 7 days of incubation. The cell cytoplasm appeared orange and the nuclei appeared purple due to ACP staining. Despite the degradation of the matrix, the osteoblasts were detected adjacent to the calcium phosphate crystals or the collagen walls (Figures 3.25 a-d). The presence of the cells after the staining process (leads to removal of inactive cells) indicates that these cells could be active in bone matrix formation.

Figure 3.25 e shows untreated, cell-free Gelfix foams stained with methylene blue-azur II revealing a highly porous structure. Comparison with Figure 3.25 f reveals the degradative effect of the incubation process on the structural integrity of the Gelfix foam.

PHBV8 foams were also stained by the same method following the embedding procedure. However, they did not take up the dyes. This might be due to insufficient penetration of the resin inside the polymeric matrix. As a result of this, the frozen sections were thicker than it was expected. Araldite sections also did not take up the dye most probably due to their thickness. However, the "optimum" foam showed, after 29 days of incubation, distinct signs of mineralization which were visible to the naked eye (100 W 10 min treated PHBV8 foam, Figure 3.26).

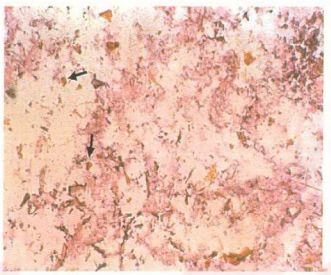

(a)

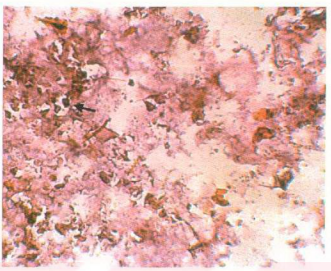

(b)

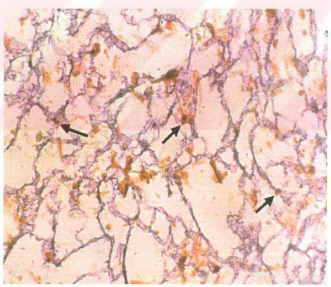

(c)

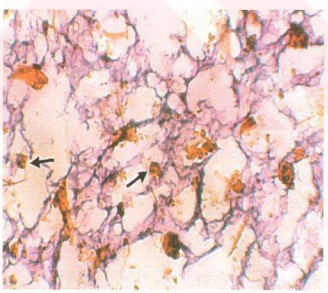

(d)

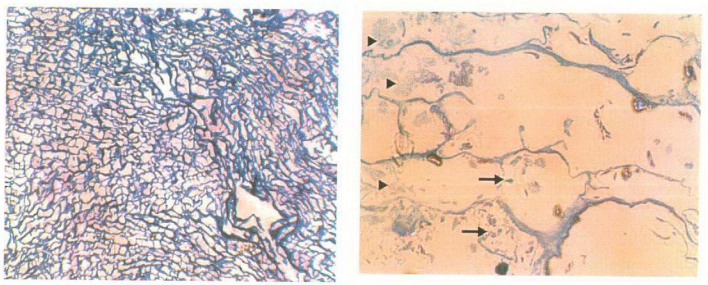

(e) (f)

Figure 3.25. Histological micrographs of Gelfix foams.

a) ACP enzyme histochemistry of calcium phosphate loaded Gelfix, Hematoxylin (x10);

b) ACP enzyme histochemistry of calcium phosphate loaded Gelfix, Hematoxylin (x20);

c) ACP enzyme histochemistry of untreated Gelfix, Hematoxylin (x10);

d) ACP enzyme histochemistry of untreated Gelfix, Hematoxylin (x20);

e) Araldite embedded semi-thin section of untreated, cell-free Gelfix, Methylene blue-azure II (x20);

f) Araldite embedded semi-thin section of calcium phosphate loaded Gelfix, Methylene blue-azure II (x10).

(Arrows indicate osteoblasts and arrow heads indicate calcium phosphate deposition)

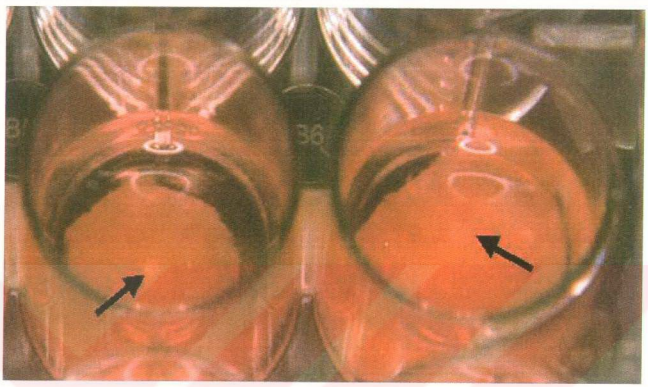

Figure 3.26. Proof of mineralization on the top surface of the rf-oxygen plasma (100 W 10 min) treated PHBV8 foam after 29 days of incubation (Arrow indicates mineralization).

3.2.2.8. Scanning Electron Microscopy

Figure 3.27 a and b shows the presence and attachment of the osteoblasts on the walls of the large sucrose loaded (300-500 μm), oxygen plasma treated (100 W 10 min) PHBV8 after 21 and 29 days of incubation in culture, respectively. Their sizes were approximately 30 μm in diameter as was expected of osteoblasts. They were found in close proximity of each other due to the initial application of the cells on small areas on the surface of the polymers. Figure 3.27 c represents the presence of a highly magnified (x750) osteoblast attached to the walls of the large sucrose loaded, untreated PHBV8 after 29 days of incubation. From these micrographs, one can not decide which incubation period is ideal for the osteoblasts because only a small fraction of the polymers were examined under the SEM.

Seven days incubated calcium phosphate loaded Gelfix's micrograph also showed the presence of the osteoblasts (Figure 3.27 d). Although the amount of the cells was higher than those of 21 and 29 days incubated PHBV8, it can not be decisively concluded that Gelfix is a better matrix material for osteoblast growth because the size of the area examined was not sufficient. In these aspects biochemical and histochemical data are expected to be more conclusive.

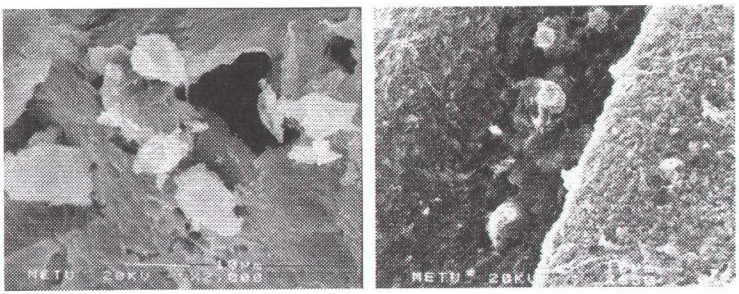

(a) (b)

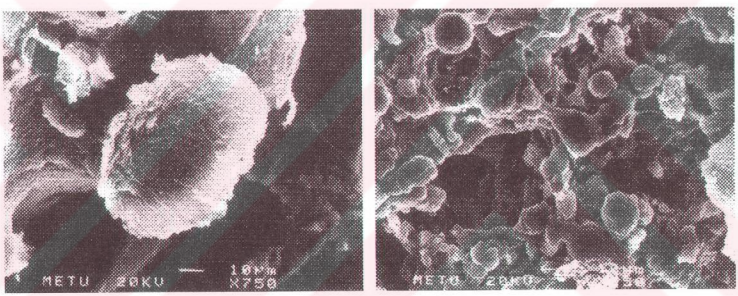

(c) (d)

Figure 3.27. Scanning electron micrographs of osteoblasts on PHBV8 and Gelfix foams: a) 21 days of incubation of osteoblasts on large sucrose loaded (300-500 μm), oxygen plasma treated (100 W 10 min) PHBV8, b) 29 days of incubation of osteoblasts on large sucrose loaded, oxygen plasma treated PHBV8, c) 29 days of incubation of osteoblasts on large sucrose loaded, untreated PHBV8, d) 7 days of incubation of osteoblasts on calcium phosphate loaded Gelfix.

3.2.2.9. Confocal Microscopy

Confocal microscopy can be used to study cell morphology, to analyze the intracellular location of various cell components, to study the migration and the spreading of the cells, the cytoskeleton and the focal adhesions, and to study apoptosis. In this study, the mineralized parts of the bone matrix produced by the osteoblasts were studied with confocal microscopy.

Figure 3.28 a and b shows that after 21 days of incubation, osteoblasts started mineralization inside the PHV8 matrices. After 29 days of incubation, degree of mineralization was increased in both untreated and oxygen plasma treated PHBV8 (Figure 3.29). As the incubation time increased, the degree of mineralization was also increased and it was higher in oxygen plasma treated cell free PHBV8 than in untreated PHBV8. Untreated and oxygen plasma treated PHBV8 foams were also dyed with tetracyclin to observe whether there was any interference (staining) due to the matrices. No significant interference could be detected. All empty matrices did not show any florescence.

Untreated and calcium phosphate loaded foams were also observed for degree of mineralization. However, due to the fast degradation of the foam, cells were only incubated for 7 days in those foams and this duration was not sufficient for mineralization.

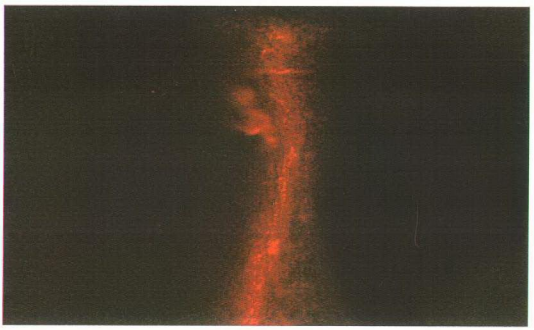

(a)

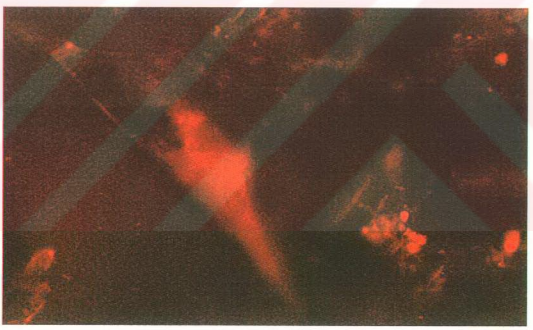

(b)

Figure 3.28. Confocal micrographs of PHBV8 foams after 21 days of incubation. PHBV8 preparation : a) untreated (x 20); b) oxygen plasma treated (100 W 10 min) (x 20).

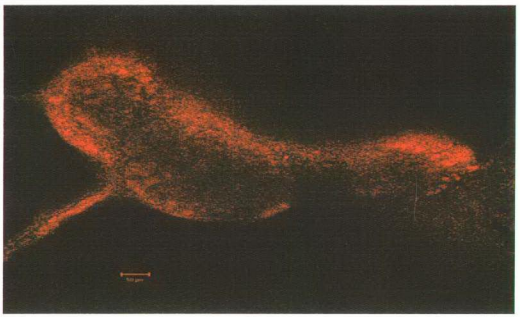

(a)

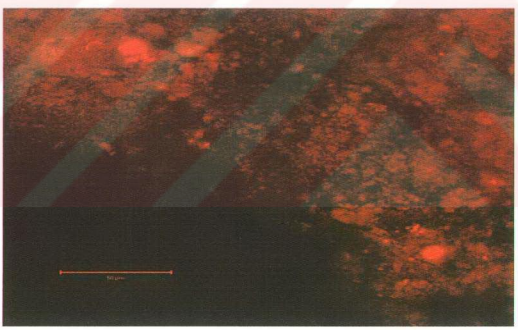

(b)

Figure 3.29. Confocal micrographs of PHBV8 foams after 29 days of incubation. PHBV8 preparation : a) untreated (x 20); b) oxygen plasma treated (100 W 10 min) (x 20).

CHAPTER 4

CONCLUSION

PHBV8 and calcium phosphate loaded collagen are very promising biodegradable matrix materials for tissue engineering applications. They were chosen as a temporary substrate or cell carrier or scaffold for osteoblast growth.

Collagen was loaded with calcium phosphate to create a composition similar to that of bone and prevent rapid degradation. The ratio of calcium over phosphate was found to be 2.26 by SEM-EDS in collagen-calcium phosphate matrix. It did not closely mimic the natural bone mineral but it is much more durable than the alternative collagen based construct. In order to obtain optimum cell growth, surface characteristics of those matrix materials were changed. The surfaces of PHBV8 foams were rendered hydrophilic by oxygen plasma treatment with the expectation of an increase in the reattachment of osteoblasts. Power and duration was changed during plasma treatment. It was also observed that plasma treatment exposed the otherwise covered voids left behind by the solute leached. This enabled a higher volume of foam to be available for cell proliferation. Thus plasma proved its worth both by modifying the surface and also by revealing the voids.

Void volume and density of the various foams were determined. SEM and Scion Image Analysis Program were used to observe the surface characteristics, average pore size and pore size distribution of PHBV8 and collagen matrices. Degradation profile of PHBV foams in aqueous media was studied. Data indicates that the microenvironment of the loaded cells will become less restrictive as time progresses and, therefore, increases in cell numbers will not be excessively hindered by space limitation.

Characterization of osteoblasts was carried out by light microscop, ALP activity determination, osteocalcin assays, and western blots for integrin. Cells exhibited spindle-like morphology and had a cell diameter of 10-30 μm as was expected. The presence of bone specific ALP and osteocalcin indicate osteoblastic cell growth. All cell passages expressed high alkaline phosphatase and osteocalcin activities. It was observed that increase in serial passage number resulted in a decrease in ALP (from 395 to 130 U/L) and osteocalcin activity (from 80 to 39 ng/cell, $x10^{-6}$). Second passage gave the best results in terms of both ALP and osteocalcin activities. Western blot data showed the presence of integrin β_1 that is also one of the indicators of osteoblast phenotype. Population doubling time of the cells was found as 50 ± 2 h. All the results proved that these cells are osteoblasts. After cell seeding onto the foams, MTS assay was carried out to determine the cell density inside the matrices. It was found that large size sucrose (300-500 μm) loaded PHBV8 (6 %, w/w) foams treated with 100 W 10 min are the optimal scaffold materials.

Osteoblast growth inside the matrices were also determined by ALP, osteocalcin assays, western blots for integrin and SEM. They all showed the presence

of osteoblasts inside the matrices. Histological evaluations and confocal microscopy showed that osteoblasts could grow inside the matrices and lead to mineralization. Also it was found that PHBV8 is a better support matrix for osteoblasts than collagen because of the rapid resorption problem associated with the latter especially in unmodified form.

This strategy offers many of the advantages of cadaver bone grafting while avoiding the complications of immune rejection, donor site morbidity, and limited availability. It thus appears that tissue engineering of bone using PHBV matrices has a serious potential.

FUTURE PROSPECTS

In vivo experiments are planned to observe bone tissue formation in Wistar rat bone defects using the implants developed in this study. The presence of the bone cells, the degree of mineralization and bone tissue formation on and inside the implants will be determined by histological examinations, SEM and confocal microscopy studies.

Depending on the results of *in vivo* experiments, surface treatment conditions, porosities or the preparation concentration of the PHBV8 and Gelfix foams will be optimized. In order to improve the seeding levels, seeding with the use of hydrogel carriers such as alginate and chondroitin sulfate are also planned.

In the final stage, mechanical property (bending and compression) of healing bone will be determined to quantify the level of healing and thus the success of the implant.

REFERENCES

Bader, A., Schilling, T., and Teebben, O.F. 1998. Tissue engineering of heart valves-human endothelial cell seeding of detergent decellularized porcine valves, *Eur. J. Cardiothorac. Surg.* 14: 279-284.

Beck, L.S., DeGuzman, L., and Lee, W.P. 1991. TGF-β1 induces bone closure of skull defects, *J.Bone Min.Res.* 6: 61257-1265.

Beck, L.S., DeGuzman, L., Lee, W.P.,. Xu, Y., Siegel, M.W., and Amento, E.P. 1993. One systemic administration of TGF-β1 reverses age- or glucocorticoid-impaired wound healing, *J.Clin.Invest.* 92: 2841-2849.

Behravesh, E., Yasko, A.W., Engel, P.S., and Mikos, A.G. 1999. Synthetic biodegradable polymers for orthopedic applications, *Clinical Orthop.and Related Res.* 367S: S118-S125.

Bostman, O., Hirvensalo, E., and Markmen, J. 1990. Foreign body reactions to fracture fixation implants of biodegradable synthetic polymers, *J.Bone Joint Surg.Br.* 2: 592-596.

Buckholz, R.W. 1987. Clinical experience with bone graft substitutes, *J.Orthop.Trauma* 3: 260-262.

Buckwalter, J.A, Glimcher, M.J., Cooper, R.R., and Recker, R. 1995. Bone biology: structure, blood supply, cells, matrix, and mineralization, *The J.Bone and Joint Surg.* 77A: 1256-1275.

Buckwalter, J.A., Glimcher, M.J., Cooper, R.R., and Recker, R. 1995. Bone biology: formation, form, modeling, remodeling, and regulation of cell functions, *The J.Bone and Joint Surg.* 77A: 1276-1287.

Canalis, E. 1988. Bone-related growth factors, *Triangle* 27: 11-20.

Cha, Y., and Pitt, C.G. 1990. The biodegradability of polyester blends, *Biomaterials* 11: 108-112.

Chapman, M.W., Bucholz, R., and Cornell, C. 1997. Treatment of acute fractures with a collagen-calcium phosphate graft material: A randomized clinical trial, *J.Bone.Joint Surg.Am.* 79: 495-502.

Coelho, M.J., and Fernandes, M.H. 2000. Human bone cell cultures in biocompatibility testing. Part II: effect of ascorbic acid, β-glycerophosphate, and dexamethasone on osteoblastic differentiation, *Biomaterials* 21: 1095-1102.

Cornell, C.N., Lane, J.M., and Chapman, M. 1991. Multicenter trial of Collograft as bone graft substitute, *J.Orthop.Trauma* 5: 1-8.

Desilets, C.P., Marden, L.J., Patterson, A.L., and Hollinger, J.O. 1990. Development of synthetic bone-repair materials for craniofacial reconstruction, *J.Craniofac.Surg.* 1: 150-153.

Du, C., Cui, F.Z., Zhu, X.D., and de Groot, K. 1999. Three dimensional nano-HAp/collagen matrix loading with osteogenic cells in organ culture, *J.Biomed.Mater.Res.* 44: 407-415.

Fleming, J.E., Cornell, C.N., and Muschler, G.F. 2000. Bone cells and matrices in orthopedic tissue engineering, *Orthop.Clinics of North America* 31: 357-374.

Freed, L.E., and Vunjak-Novakovic, G. 1998. Culture of organized cell communities, *Adv. Drug Delivery Rev.* 33: 15-30.

Frost, H. 1991. A new direction for osteoporosis research: A review and proposal, *Bone* 12: 429-437.

Fukada, E., and Ando, Y. 1986. Piezoelectric properties of Poly-β-hydroxybutyrate and copolymers of β-hydroxybutyrate and β-hydroxyvalerate, *Int.J.Biol.Macromol.* 8: 361-366.

Galego, N., Rozsa, C., Sanchez, R., Fung, J., Vazquez, A., and Tomas, J.S. 2000. Characterization and application of poly(β-hydroxyalkanoates) family as composite biomaterials, *Polymer Testing* 19: 485-492.

Ganta, G., Pastizzo, G., McCarthy, M., and Gronowicz, G. 1994. Ascorbic acid deficiency inhibits integrin expression prior to its effect on collagen synthesis in fetal rat parietal bone cultures, *J.Bone Miner.Res.* 9: S254.

Gao, T.J., Lindholm, T.S., Marttinen, A., and Puolakka, T. 1993. Bone inductive potential and dose-dependent response of bovine bone morphogenetic protein combined with type IV collagen carrier, *Ann..Chir.Gynaecol.* 82: 77-84.

Gassner, F., and Owen, A.J. 1996. Some properties of poly(3-hydroxybutyrate-co-3-hydroxyvalerate) blends, *Polymer. Intern.* 39: 215-219.

Gazdag, A.R., Lane, J.M., and Glaser, D. 1995. Alternatives to autogenous bone graft: Efficacy and indications, *J.Am.Acad.Orthop.Surg.* 3: 1-8.

Gerhart, T.N., Roux, R.D., Horowitz, G., Miller, R.L., Hanff, P., and Hayes, W.C. 1988. Antibiotic release from an experimental biodegradable bone cement, *J.Orthop.Res.* 6: 585-592.

Glowacki, J., and Mulliken, J.B. 1985. Demineralized bone implants, *Clin.Plast.Surg.* 12: 233.

Gogolewski, S., Jovanovic, M., Perren, S.M., Dillon, J.G., and Hughes, M.K. 1993. Tissue response and *in vivo* degradation of the selected polyhydroxyacids: Polylactides (PLA), poly(3-hydroxybutyrate) (PHB), and poly(3-hydroxybutyrate-co-3- hydroxyvalerate) (PHB/VA), *J.Biomed. Mater. Res.* 27: 1135-1148.

Goldberg, V.M., Stevenson, S., and Shaffer, J.W. 1991. Biology of autografts and allografts: In bone and cartilage allografts, *American Academy of Orthopedic Surg. Symposium,* Park Ridge, IL, pp. 3-13.

Gombotz, W.R., Pankey, S.C., Ranchalis, L.S., and Puolakkainen, P. 1993. Controlled release of TGF-β1 from a biodegradable matrix for bone regeneration, *J. Biomater. Sci. Polym. Edn.* 5: 49-63.

Göpferich, A. 1996. Mechanisms of polymer degradation, *Biomaterials* 17: 103-114.

Gürsel, İ., Korkusuz, F., Türesin, F., Alaeddinoğlu, N.G., and Hasırcı, V. 2001. In vivo application of biodegradable controlled antibiotic release systems for the treatment of implant- related osteomyelitis, *Biomaterials* 22: 73-80.

Hasırcı, V., Lewandrowski, K., Bondre, S.P., Gresser, J.D., Trantolo, D.J., and Wise, D.L. 2000. High strength bioresorbable bone plates: preparation, mechanical properties, and *in vitro* analysis, *Bio-medical Materials and Engineering* 10: 19-29.

Holmes, R., Bucholz, R., and Mooney, V. 1986. Porous hydroxyapatite as a bone graft substitute in metaphyseal defects, *J.Bone Joint Surg.Am.* 68: 904-911.

Hsu, F.Y., Chueh, S.C., and Wang, Y.J. 1999. Microspheres of hydroxyapatite /reconstituted collagen as supports for osteoblast cell growth, *Biomaterials* 20: 1931-1936.

Ingber, D. 1993. Extracellular matrix: Cellular mechanics and tissue engineering, Birkhauser, Basel, Berlin, pp. 69-83.

Ishaug, S.L., Crane, G.M., Miller, M.J., Yasko, A.W., Yaszemski, M.J., and Mikos, A.G. 1997. Bone formation by three-dimensional stromal osteoblast culture in biodegradable polymer scaffolds, *J.Biomed.Mater.Res.* 36: 17-28.

Ishaug, S.L., Yaszemski, M.J., Bizios, R., and Mikos, A.G. 1994. Osteoblast function on synthetic biodegradable polymers, *J.Biomed.Mater.Res.* 28: 1445-1453.

Jupiter, J.B., Winters, S., and Sigman, S. 1997. Repair of five distal radius fractures with an investigational bone cement: A preliminary report, *J.Orthop.Trauma* 11: 110-116.

Khan, S.N., Tomin, E., and Lane, J.M. 2000a. Clinical applications of bone graft substitutes, *Orthop.Clinics of North America* 31: 389-398.

Khan, S.N., Bostrom, M.P.G., and Lane, J.M. 2000b. Bone growth factors, *Orthop.Clinics of North America* 31: 375-387.

Koosha, F., Muller, R.H., and Davis, S.S. 1989. Polyhydroxybutyrate as a drug carrier, *Cri.Rev.Therap.Drug Carr.Sys.* 6: 117-130.

Langer, R. 1997. Tissue engineering: A new field and its challenges, *Pharmaceutical Research* 14: 840-841.

Lemmouchi, Y., Schacht, E., and Lootens, C. 1998. *In vitro* release of try-panocidal drugs from biodegradable implants based on poly(epsilon-caprolactone) and poly(D,L-lactide), *J. Controlled Release* 55: 79–85.

Liebergall, M., Young, R.G., Ozawa, N., Reese, J.H., Davy, D.T., Goldberg, V.M., and Caplan, A.I. 1994. The effects of cellular manipulation and TGF-β in a composite bone graft. In: Bone Formation and Repair, Brighton CT, Friedlaende GE, Lane JM, eds., Rosemont, IL: American Academy of Orthopedic Surgeons.

Lowry, K.J., Hamson, K.R., Bear, L., Peng, Y.B., Calaluce, R., Evans, M.L., Anglen, J.O., and Allen, W.C. 1997. Polycaprolactone/glass bioabsorbable implant in a rabbit humerus fracture model, *J. Biomed. Mater. Res.* 36: 536–541.

Lu, L., Garcia, C.A., and Mikos, A.G. 1998. Retinal pigment epithelium cell culture on thin biodegradable poly(DL-lactic-co-glycolic acid) films, *J. Biomater. Sci. Res. Polymer Ed.* 9: 1187-1205.

Luklinska, Z.B., and Bonfield, W. 1997. Morphology and ultrastructure of the interface between hydroxyapatite-polyhydroxybutyrate composite implant and bone, *J. Mater. Sci. Mater in Med.* 8: 379-383.

Maniatopoulos, C., Sodek, J., and Melcher, A. 1988. Bone formation *in vitro* by stromal cells obtained from bone marrow of young adult rats, *Cell Tissue Res.* 254: 317-330.

Mitomo, H., Barham, P.J., and Keller, A. 1987. Crystallization and morphology of poly(β-hydroxybutyrate) and its copolymer, *Polymer J.* 19: 1241-1253.

Miyamoto, S., and Takaoka, K. 1993. Bone induction and bone repair by composites of bone morphogenetic protein and biodegradable synthetic polymers, *Ann. Chir. Gynaecol.* 82: 69-75.

Mooney, D.J., and Mikos, A.G. 1999. Growing new organs, *Scientific American* 280: 60-65.

Muller, H.M., and Seebach, D. 1993. Poly(hydroxyalkanoates), A fifth class of physiologically important organic biopolymers, *Angew. Chem. Int. Engl.* 32: 477-502.

Nichter, R.S., Yazdi, M., Kosari, K., Sridjaja, R., Ebramzadeh, E., and Nimni, M.E. 1992. Demineralized bone matrix polydioxanone composite as a substitute for bone graft: a comparative study in rats, *J.Craniofac.Surg.* 3: 63-69.

Nielsen, F., Karring, T., and Gogolewski, S. 1992. Biodegradable guide for bone regeneration. Polyurethane membranes tested in rabbit radius defects, *Acta Orthop.Scand.* 63: 66-69.

Peter, S.J., Lu, L., Kim, D.J., and Mikos, A.G. 2000. Marrow stromal osteoblast function on a poly(propylene fumarate)/β-tricalcium phosphate biodegradable orthopaedic composite, *Biomaterials* 21: 1207–1213.

Peter, S.J., Miller, S.T., Zhu, G., Yasko, G., and Mikos, A.G. 1998. *In vivo* degradation of a poly(propylene fumarate)/β-tricalcium phosphate injectable scaffold, *J. Biomed. Mater. Res.* 41: 1–7.

Peter, S.J., Yaszemski, M.J., Suggs, L.J., Payne, R.G., Langer, R., Hayes, W.C., Unroe, M.R., Alemany, L.B., Engel, P.S., and Mikos, A.G. 1997. Characterization of partially saturated poly(propylene fumarate) for orthopaedic application, *J. Biomater. Sci. Polym. Ed.* 8: 893–904.

Peyman, G.A., Yang, D., Khoobehi, B., Rahimy, M.H. and Chin, S.Y. 1996. *In vitro* evaluation of polymeric matrix and porous biodegradable reservoir devices for slow-release drug delivery, *Ophthal. Surg. Lasers* 27: 384–391.

Pitt, C.G., and Gu, Z.W. 1987. Modification of the rates of chain cleavage of poly(ε-caprolactone) and related polyesters in the solid state, *J. Controlled Release* 4: 292–293.

Pitt, C.G., Bao, Y.T., Andrady, A.L., and Samuel, P.N.K. 1988. The correlation of polymer water and octanol-water partition coefficients: estimation of drug solubilities in polymers, *Int. J. Pharm.* 45: 1–11.

Pitt, C.G., Gratzl, M.M., Kimmel, G.L., Surles, J., and Schindler, A. 1981. Aliphatic Polyesters II. The degradation of poly(DL-lactide), poly(ε-caprolactone), and their copolymers *in vivo*, *Biomaterials* 2: 215–220.

Pollok, J.M., and Vacanti, J.P. 1996. Tissue engineering, *Seminars in Pediatric Surgery* 5: 191-196.

Pouton, C.W., and Akhtar, S. 1996. Biosynthetic polyhydroxyalkanoates and their potential in drug delivery, *Adv.Drug.Del.Rev.* 18: 133-162.

Pulapura, S.,and Kohn, J. 1992. Trends in the development of bioresorbable polymers for medical applications, *J. Biomater. Applic.* 6: 216-249.

Rader, C.P., Keller, H.W., and Rehm, K.E. 1992. Surgical treatment of dislocated 3 and 4-segment fractures of the proximal humerus, *Unfallchirurg* 95: 613-617.

Raisz, L.G. 1988. Bone metabolism and its hormonal regulation: An update, *Triangle* 27: 5-10.

Reusch, R.N. 1995. Low molecular weight complexed poly(3-hydroxybutyrate): a dynamic and versatile molecule in vivo, *Can. J. Microbiol.* 41: 50-54.

Rivard, C.H., Chaput, C., Rhalmi, S., and Selmani, A. 1996. Bio-absorbable synthetic polyesters and tissue regeneration. A study of three-dimensional proliferation of ovine chondrocytes and osteoblasts, *Ann.Chir.* 50: 651-658.

Saad, B., Neunenschwander, P., Uhlschmid, G.K., and Suter, U.W. 1999. New versatile, elastomeric, degradable polymeric materials for medicine, *Int.J.Biol.Macromolecules* 25: 293-301.

Saito, T., Albelda, S., and Brighton, C. 1994. Identification of integrin receptors on cultured human bone cells, *J.Orthop.Res.* 12: 384-394.

Saltzman, W.M. 1996. Growth-factor delivery in tissue engineering, *MRS Bulletin* 21: 62-65.

Seal, B.L., Otero, T.C., and Panitch, A. 2001. Polymeric biomaterials for tissue and organ regeneration, *Materials Science and Eng. R.* 34: 147-230.

Solchaga, L.A., Dennis, J.E., Goldberg, V.M., and Caplan, A.I. 1999. Hyaluronic acid-based polymers as cell carriers for tissue engineered repair of bone and cartilage, *J.Orthop.Res.* 17: 205-213.

Solheim, E. 1998. Growth factors in bone, *Int.Orthop.* 22: 410-416.

Strates, B.S., Kilaghbran, V., Nimni, M.E., and McGuire, M.H. 1992. Enhanced periostal osteogenesis induced by TGF-β1 adsorbed on microcrystals of hydroxyapatite, *Trans.Orthop.Res.Soc.* 591.

Sumner, D.R., Turner, T.M., Purchio, A.F., Gombotz, W.R.,.Urban, R.M., and Galante, J.O. 1995. Enhancement of bone ingrowth by TGF-β, *J.Bone Joint.Surg.* 77A: 1135-1147.

Takahata, H., Lavelle, E.C., Coombes, A.G.A., and Davis, S.S. 1998. The distribution of protein associated with poly(DL-lactide-co-glycolide) microparticles and its degradation in stimulated body fluids, *J. Contr. Rel.* 50: 237-246.

Takaoka, K., Nakahara, H., Yoshikawa, H., Masuhara, K., Tsuda, T., and Ono, K. 1988. Ectopic bone induction on and in porous hydroxyapatite combined with collagen and bone morphogenetic protein, *Clin.Orthop.Rel.Res.* 234: 250-254.

Tiedeman, J.J., Garvin, K.L., and Kile, T.A. 1995. The role of composite, demineralized bone marrow in the treatment of osseous defects, *Orthopedics* 18: 1153-1158.

Turner, T.M., Urban, R.M., and Gitelis, S. 1999. Efficacy of calcium sulphate, a synthetic bone graft material, in healing a large canine medullary defect, *Trans.ORS* 24: 522.

Urist, M.R. 1965. Bone: Formation by autoinduction, *Science* 150: 893-899.

Uyama, H., and Kobayashi, S. 1994. Enzymatic ring-opening polymerization of lactose catalyzed by lipase, *Poly. Prepr.* 35, 444–445.

Vacanti, C.A., Kim, W., Upton, J., Mooney, D., and Vacanti, J.P. 1995. The efficacy of periosteal cells compared to chondrocytes in the tissue engineered repair of bone defects, *Tissue Eng.* 1: 301-308.

Vacanti, J.P., and Langer, R. 1999. Tissue engineering: The design and fabrication of living replacement devices for surgical reconstruction and transplantation, *Lancet.* 34: S132-134.

von Recum, H.A., Cleek, R.L., Eskin, S.G., and Mikos, A.G. 1995. Degradation of polydispersed poly(L-lactic acid) to modulate lactic acid release, *Biomaterials* 16: 441-447.

Yamada, K.M., and Miyamoto, S. 1995. Integrin transmemebrane signaling and cytoskeletal control, *Curr. Opin Cell Biol.* 7: 681-689.

Yamazaki, Y., Oida, S., Akimoto, Y., and Shioda, S. 1988. Response of the mouse femoral muscle to an implant of a composite of bone morphogenetic protein and plaster of Paris, *Clin.Orthop.Rel.Res.* 234: 240-249.

Yasko, A.W., Lane, J.M., Fellinger, E.J., Rosen, V., Wozney, J.M., and Wang, E.A. 1992. The healing of segmental bone defects induced by recombinant human bone morphogenetic protein (rhBMP-2): a radiographic, histological, and biomechanical study in rats, *J.Bone Joint Surg.* 74A: 659-670.

Yaszemski, M.J., Payne, R.G., Hayes, W.C., Langer, R., and Mikos, A.G. 1996a. Evaluation of bone transplantation: molecular, cellular and tissue strategies to engineer human bone, *Biomaterials* 17: 175-185.

Yaszemski, M.J., Payne, R.G., Hayes, W.C., Langer, R., and Mikos, A.G. 1996b. The in vitro degradation of a poly(propylene fumarate)-based composite material, *Biomaterials* 17: 2127-2130.

Yaszemski, M.J., Payne, R.G., Hayes, W.C., Langer, R.S., Aufdemorte, T.B., and Mikos, A.G. 1995. The ingrowth of new bone tissue and initial mechanical properties of a degradable polymeric composite scaffold, *Tissue Eng.* 1: 41–52.

Yaylaoğlu, M.B., Yıldız, C., Korkusuz, F., and Hasırcı, V. 1999. Novel osteochondral implant, *Biomaterials* 20: 1513-1520.

Zerwekh, J.E., Kourosh, S., and Schienbergt, R. 1992. Fibrillar collagen-biphasic calcium phosphate composite as a bone graft substitute for spinal fusion, *J.Orthop.Res.* 10: 562-572.

APPENDIX A

CALCULATION OF FOAM DENSITY

An empty pycnometer was weighed (w_o). It was weighed again after completely filling with distilled water (w_1). Then, a previously weighed (w_f) foam was placed into the pycnometer which was filled with distilled water and weighed again (w_2). The addition of foam displaced an equal volume of water. However, during this process some water was adsorbed by the foam because of its porous structure and the capillary action. Therefore, the foam was weighed again after removal from the pycnometer. All these data were used to calculate the density of foam.

For the calculation of foam density the following equations were used:

$W_{w1} = w_1 - w_o$

$W_{w2} = w_2 - w_f - w_o$

$Wr = W_{w1} - W_{w2}$

$V_w = Wr + (W_3 - W_f)$

$V_w = V_f$

$D_f = W_f / V_f$

W_{w1} : Weight of water completely filling the pycnometer

W_{w2} : Weight of water remaining inside after foam was placed in the pycnometer

W_3 : Weight of foam after removal from the pycnometer

W_r : Weight of water displaced by the foam

V_w : Volume of water displaced water which is equal to its weight

V_f : Volume of foam

D_f : Density of foam

VITA

Gamze Torun Köse was born in Ankara on May 13, 1972. She received her BSc degree from the Department of Biological Sciences of the Middle East Technical University, Ankara, Turkey in June 1994. She started her PhD studies after receiving her MSc in Biotechnology Department of the same university in September 1996. Between September 1998 and September 1999, she carried out part of her PhD studies at the University of Texas, MD Anderson Cancer Center, Department of Bioimmunotherapy and Drug Release as a predoctoral fellow. She was employed as a research assistant of the Biological Sciences Department between 1994 and 2002. Her research interests include bone and cartilage tissue engineering, cell culture techniques, stable and biodegradable biomaterials, polymers, and liposomes.